Virial coefficients of anisotropic hard solids of revolution: The detailed influence of the particle geometry

Elisabeth Herold, Robert Hellmann, and Joachim Wagner

Citation: The Journal of Chemical Physics **147**, 204102 (2017);
View online: https://doi.org/10.1063/1.5004687
View Table of Contents: http://aip.scitation.org/toc/jcp/147/20
Published by the American Institute of Physics

Virial coefficients of anisotropic hard solids of revolution: The detailed influence of the particle geometry

Elisabeth Herold, Robert Hellmann, and Joachim Wagner
Institut für Chemie, Universität Rostock, D-18051 Rostock, Germany

(Received 14 September 2017; accepted 18 October 2017; published online 22 November 2017)

We provide analytical expressions for the second virial coefficients of differently shaped hard solids of revolution in dependence on their aspect ratio. The second virial coefficients of convex hard solids, which are the orientational averages of the mutual excluded volume, are derived from volume, surface, and mean radii of curvature employing the Isihara–Hadwiger theorem. Virial coefficients of both prolate and oblate hard solids of revolution are investigated in dependence on their aspect ratio. The influence of one- and two-dimensional removable singularities of the surface curvature to the mutual excluded volume is analyzed. The virial coefficients of infinitely thin oblate and infinitely long prolate particles are compared, and analytical expressions for their ratios are derived. Beyond their dependence on the aspect ratio, the second virial coefficients are influenced by the detailed geometry of the particles. *Published by AIP Publishing.* https://doi.org/10.1063/1.5004687

I. INTRODUCTION

The interaction of hard bodies is of tremendous importance for condensed matter physics since the self-organization of matter at high volume fractions is essentially influenced by the mutual excluded volume. Although the virial series was introduced by Kamerlingh Onnes[1] originally to provide an equation of state for imperfect gases at comparatively small number densities, it later gained importance for density expansions in liquid state theory.[2–4] Moreover, the virial equation of state, due to its connection to the free energy of many-particle systems, plays an important role in classical density functional theory (DFT) used to investigate the phase behavior of condensed matter.[5,6] Although the infinite sequence of the virial equation is needed for the estimation of the free energy, the knowledge of the second virial coefficient is an essential starting point since the relation of higher virial coefficients to the second one can approximately be expressed by a recursion relation proposed by Carnahan and Starling.[7] This geometric series describes the equation of state for hard spheres surprisingly well and leads to a comparatively simple expression for the free energy. Several DFT studies concerning the phase behavior of anisotropic particles approximate the free energy via the second virial coefficient of anisotropic particles, while the Carnahan–Starling series is used for the contributions of higher virial coefficients.[8–10]

The starting point of understanding the phase behavior of anisotropic particles is the seminal work of Onsager[11] predicting an isotropic-nematic phase transition for hard spherocylinders of sufficiently large aspect ratio. Onsager derived an analytical expression for the second virial coefficient of hard spherocylinders, while analytical expressions for the virial coefficients of cylinders and prolate and oblate ellipsoids were derived by Isihara.[12] Geometric measures needed to calculate second virial coefficients of several hard convex bodies were compiled by Boublík and Nezbeda.[13] The comparison of these geometries already shows a detailed influence of the particles' geometry beyond their aspect ratio.

With the advent of computer simulations, hard anisotropic particles attracted increasing interest in recent decades. Frenkel *et al.* studied the phase behavior of hard ellipsoids by means of Monte Carlo methods.[14] In subsequent studies, the influence of additional short-range interactions was investigated.[15,16] In addition to hard oblate particles, hard platelets were also investigated by means of Monte Carlo simulations,[17] whose predictions were verified by experiments using gibbsite platelets as a model system.[18]

The availability of differently shaped colloidal model systems like spindles,[19,20] plates,[21,22] hypercubes,[23] and polyhedrons[24] has driven the interest in the phase behavior of unusually shaped hard particles.[25–30] The virial coefficients of hard ellipsoids up to the fifth order were calculated by Vega.[31]

The aim of this contribution is to provide analytical expressions for the second virial coefficients of different geometries in dependence on their aspect ratio. We show that singularities in the surface curvature of convex solids can be removed by continuously completing solids of revolution by segments of spheres or ellipsoids in the vicinity of singularities and analyzing the limit of these contributions for infinitely small sphere segments and infinitely thin ellipsoids. By this approach, analytical expressions for the second virial coefficients of different prolate and oblate solids of revolution such as double cones, spindles, lenses, cones, truncated cones, and sphere segments are accessible.

This contribution is organized as follows: in Sec. II, we calculate the volume, surface, and mean radius of curvature from the meridian curve of solids of revolution by means of differential geometry. In Sec. III, we briefly review the results for ellipsoids and spherocylinders as examples of geometries

without singularities of their surface curvature since segments of ellipsoids are needed to remove discontinuities in the derivatives of meridian curves describing solids containing singularities which might influence the mean radius of curvature. With this approach, analytical second virial coefficients for geometries containing singularities in their surface are derived. In Sec. IV, the results for different prolate and oblate geometries in dependence on their aspect ratio are compared.

II. THEORETICAL BACKGROUND

A. Second virial coefficient

The thermal equation of state of a gaseous or supercritical many-particle system can be expressed as an infinite power series in the particle number density ϱ,

$$\frac{p}{k_\mathrm{B}T} = \varrho + B_2\,\varrho^2 + B_3\,\varrho^3 + B_4\,\varrho^4 + \cdots = \varrho + \sum_{i=2}^{\infty} B_i \varrho^i\,, \quad (1)$$

where p is the pressure, T is the temperature, and k_B is Boltzmann's constant. The expansion coefficients B_i are the virial coefficients of order i.

Truncating Eq. (1) after the linear term leads to the equation of state of an ideal gas. The first contribution accounting for deviations from the ideal gas behavior is the second virial coefficient B_2, which is related to pair interactions, while contributions of higher powers in ϱ are related to three-body interactions, four-body interactions, etc.

In terms of statistical mechanics, the second virial coefficient B_2 of axially symmetric, anisotropic particles with their orientations denoted by the unit vectors $\hat{\mathbf{u}}_1$ and $\hat{\mathbf{u}}_2$ can be expressed as

$$B_2 = -\frac{1}{2V}\frac{1}{16\pi^2}\oiint_{4\pi}\oiint_{4\pi}\int_V\int_V f(\mathbf{r}_1,\hat{\mathbf{u}}_1,\mathbf{r}_2,\hat{\mathbf{u}}_2) \times d^3\mathbf{r}_1\,d^3\hat{\mathbf{u}}_1 d^3\mathbf{r}_2\,d^3\hat{\mathbf{u}}_2, \quad (2)$$

where $\mathbf{r}_1$ and $\mathbf{r}_2$ are the center-of-mass coordinates of both particles and V is the volume of the many-particle system. In Eq. (2), $f(\mathbf{r}_1,\hat{\mathbf{u}}_1,\mathbf{r}_2,\hat{\mathbf{u}}_2)$ denotes the Mayer f-function,

$$f(\mathbf{r}_1,\hat{\mathbf{u}}_1,\mathbf{r}_2,\hat{\mathbf{u}}_2) = \exp\left[-\frac{u(\mathbf{r}_1,\hat{\mathbf{u}}_1,\mathbf{r}_2,\hat{\mathbf{u}}_2)}{k_\mathrm{B}T}\right] - 1, \quad (3)$$

with the pair interaction energy $u(\mathbf{r}_1,\hat{\mathbf{u}}_1,\mathbf{r}_2,\hat{\mathbf{u}}_2)$. The interaction energy depends only on the relative particle distance $\mathbf{r}_{12} = \mathbf{r}_2 - \mathbf{r}_1$ and the inner products $\hat{\mathbf{r}}_{12}.\hat{\mathbf{u}}_1$, $\hat{\mathbf{r}}_{12}.\hat{\mathbf{u}}_2$, and $\hat{\mathbf{u}}_1.\hat{\mathbf{u}}_2$ as rotational invariants with $\hat{\mathbf{r}}_{12}$ denoting a unit vector in the direction of the interdistance $\mathbf{r}_{12}$. Hence, we can choose $\mathbf{r}_1$ as the coordinate system's origin and obtain with $f(\mathbf{r}_1,\hat{\mathbf{u}}_1,\mathbf{r}_2,\hat{\mathbf{u}}_2) = f(\mathbf{r}_{12},\hat{\mathbf{u}}_1,\hat{\mathbf{u}}_2)$ and by performing the trivial integration over $d^3\mathbf{r}_1$ (yielding the volume V),

$$B_2 = -\frac{1}{2}\frac{1}{16\pi^2}\oiint_{4\pi}\oiint_{4\pi}\int_V f(\mathbf{r}_{12},\hat{\mathbf{u}}_1,\hat{\mathbf{u}}_2)\,d^3\mathbf{r}_{12}\,d^3\hat{\mathbf{u}}_1 d^3\hat{\mathbf{u}}_2 = -\frac{1}{2}\int_V \langle f(\mathbf{r}_{12},\hat{\mathbf{u}}_1,\hat{\mathbf{u}}_2)\rangle_{\hat{\mathbf{u}}_1,\hat{\mathbf{u}}_2}\,d^3\mathbf{r}_{12}. \quad (4)$$

Hence, the second virial coefficient is proportional to the integral over the canonical orientation average of the Mayer f-function.

For particles interacting via hard-body exclusion, the potential and the resulting Mayer f-function can be written as

$$u(\mathbf{r}_{12}) = \begin{cases} \infty : |\mathbf{r}_{12}| \le r_c(\hat{\mathbf{r}}_{12},\hat{\mathbf{u}}_1,\hat{\mathbf{u}}_2) \\ 0 \;\; : |\mathbf{r}_{12}| > r_c(\hat{\mathbf{r}}_{12},\hat{\mathbf{u}}_1,\hat{\mathbf{u}}_2) \end{cases}, \quad (5a)$$

$$f(\mathbf{r}_{12}) = \begin{cases} -1 : |\mathbf{r}_{12}| \le r_c(\hat{\mathbf{r}}_{12},\hat{\mathbf{u}}_1,\hat{\mathbf{u}}_2) \\ 0 \;\; : |\mathbf{r}_{12}| > r_c(\hat{\mathbf{r}}_{12},\hat{\mathbf{u}}_1,\hat{\mathbf{u}}_2) \end{cases}, \quad (5b)$$

where $r_c(\hat{\mathbf{r}}_{12},\hat{\mathbf{u}}_1,\hat{\mathbf{u}}_2)$ denotes the contact distance of the configuration with the orientations $\hat{\mathbf{u}}_1$ and $\hat{\mathbf{u}}_2$ and the direction $\hat{\mathbf{r}}_{12}$ of the distance vector. The determination of contact distances r_c of arbitrarily shaped objects is a nontrivial problem.

B. Isihara–Hadwiger theorem

Isihara[12,32,33] and Hadwiger[34] have independently shown that the second virial coefficient of hard convex bodies can be determined analytically from the volume V_P, the surface S_P, and the mean radius of curvature $\tilde{R}_\mathrm{P}$ of the particle. The latter quantity is the reciprocal of the integral mean curvature H_P. The second virial coefficient B_2 of convex bodies can, employing the Isihara–Hadwiger theorem, be written as

$$B_2 = V_\mathrm{P} + \tilde{R}_\mathrm{P} S_\mathrm{P}. \quad (6)$$

For hard bodies, the second virial coefficient B_2 is the orientational average of the mutual excluded volume. Since the dimension of the second virial coefficient is a volume, a reduced second virial coefficient can be defined as

$$B_2^* = \frac{B_2}{V_\mathrm{P}} = 1 + \frac{\tilde{R}_\mathrm{P} S_\mathrm{P}}{V_\mathrm{P}}. \quad (7)$$

The quantities V_P, $\tilde{R}_\mathrm{P}$, and S_P in Eq. (6) can be calculated analytically by methods of differential geometry if the meridian curve $r(z)$ of a solid of revolution is known.

Let us parameterize the surface of an axially symmetric solid of revolution as

$$\Psi(\varphi, z) = \begin{pmatrix} r(z)\,\cos\varphi \\ r(z)\,\sin\varphi \\ z \end{pmatrix} \quad (8)$$

with the meridian curve $r(z)$ and the azimuth φ. Its volume is given by

$$V_\mathrm{P} = \int \pi r^2(z) dz. \quad (9)$$

The surface is

$$S_\mathrm{P} = \int 2\pi r(z)\,ds \quad (10)$$

with the arc length $ds = \left\{[dr(z)]^2 + [dz]^2\right\}^{1/2}$, which can be written as

$$ds = \left\{\left[\frac{dr(z)}{dz}\right]^2 + 1\right\}^{1/2} dz = \left[\dot{r}^2(z) + 1\right]^{1/2} dz, \quad (11)$$

resulting in

$$S_\mathrm{P} = 2\pi \int r(z)\left[\dot{r}^2(z) + 1\right]^{1/2} dz. \quad (12)$$

The mean curvature H_P can be obtained from the trace of the Weingarten tensor $\underline{\underline{\mathcal{W}}}$,

$$H_\mathrm{P} = \frac{1}{2}\mathrm{Tr}\left(\underline{\underline{\mathcal{W}}}\right) = \frac{1}{2}\mathrm{Tr}\left(\underline{\underline{\mathbf{I}}}_\mathrm{P}^{-1}\,\underline{\underline{\mathbf{II}}}_\mathrm{P}\right), \tag{13}$$

where the tensors $\underline{\underline{\mathbf{I}}}_\mathrm{P}$ and $\underline{\underline{\mathbf{II}}}_\mathrm{P}$ are the first and second fundamental form of the particle's surface $\Psi(\varphi, z)$. The fundamental forms are

$$\underline{\underline{\mathbf{I}}}_\mathrm{P} = \begin{bmatrix} \left(\frac{\partial\Psi}{\partial\varphi}\right)\cdot\left(\frac{\partial\Psi}{\partial\varphi}\right) & \left(\frac{\partial\Psi}{\partial\varphi}\right)\cdot\left(\frac{\partial\Psi}{\partial z}\right) \\ \left(\frac{\partial\Psi}{\partial z}\right)\cdot\left(\frac{\partial\Psi}{\partial\varphi}\right) & \left(\frac{\partial\Psi}{\partial z}\right)\cdot\left(\frac{\partial\Psi}{\partial z}\right) \end{bmatrix} \tag{14}$$

and

$$\underline{\underline{\mathbf{II}}}_\mathrm{P} = \begin{bmatrix} \hat{\mathbf{n}}\cdot\left(\frac{\partial^2\Psi}{\partial\varphi^2}\right) & \hat{\mathbf{n}}\cdot\left(\frac{\partial^2\Psi}{\partial\varphi\partial z}\right) \\ \hat{\mathbf{n}}\cdot\left(\frac{\partial^2\Psi}{\partial z\partial\varphi}\right) & \hat{\mathbf{n}}\cdot\left(\frac{\partial^2\Psi}{\partial z^2}\right) \end{bmatrix}, \tag{15}$$

where $\hat{\mathbf{n}} \equiv \hat{\mathbf{n}}(\varphi, z)$ denotes the normal field,

$$\hat{\mathbf{n}}(\varphi, z) = \frac{\left(\frac{\partial\Psi}{\partial\varphi}\right)\times\left(\frac{\partial\Psi}{\partial z}\right)}{\left\|\left(\frac{\partial\Psi}{\partial\varphi}\right)\times\left(\frac{\partial\Psi}{\partial z}\right)\right\|}, \tag{16}$$

of the particle surface. With the first derivatives

$$\left(\frac{\partial\Psi}{\partial\varphi}\right) = \begin{pmatrix} -r(z)\,\sin\varphi \\ r(z)\,\cos\varphi \\ 0 \end{pmatrix}, \tag{17a}$$

$$\left(\frac{\partial\Psi}{\partial z}\right) = \begin{pmatrix} \dot{r}(z)\,\cos\varphi \\ \dot{r}(z)\,\sin\varphi \\ 1 \end{pmatrix}, \tag{17b}$$

the normal field of a solid's of revolution surface can be written as

$$\hat{\mathbf{n}}(\varphi, z) = \frac{1}{\left(1+\dot{r}^2(z)\right)^{1/2}}\begin{pmatrix} \cos\varphi \\ \sin\varphi \\ -\dot{r}(z) \end{pmatrix}. \tag{18}$$

Employing the same derivatives, the first fundamental form results in

$$\underline{\underline{\mathbf{I}}}_\mathrm{P} = \begin{pmatrix} r^2(z) & 0 \\ 0 & 1+\dot{r}^2(z) \end{pmatrix}. \tag{19}$$

Since the first fundamental form is a diagonal matrix, its inverse can directly be written as

$$\underline{\underline{\mathbf{I}}}_\mathrm{P}^{-1} = \begin{pmatrix} \frac{1}{r^2(z)} & 0 \\ 0 & \frac{1}{1+\dot{r}^2(z)} \end{pmatrix}. \tag{20}$$

With the second derivatives

$$\frac{\partial^2\Psi}{\partial\varphi^2} = \begin{pmatrix} -r(z)\cos\varphi \\ -r(z)\sin\varphi \\ 0 \end{pmatrix}, \tag{21a}$$

$$\frac{\partial^2\Psi}{\partial\varphi\partial z} = \begin{pmatrix} -\dot{r}(z)\sin\varphi \\ \dot{r}(z)\cos\varphi \\ 0 \end{pmatrix}, \tag{21b}$$

$$\frac{\partial^2\Psi}{\partial z^2} = \begin{pmatrix} \ddot{r}(z)\cos\varphi \\ \ddot{r}(z)\sin\varphi \\ 0 \end{pmatrix}, \tag{21c}$$

and the normal field $\hat{\mathbf{n}}(\varphi, z)$, the diagonal matrix

$$\underline{\underline{\mathbf{II}}}_\mathrm{P} = \frac{1}{\left(1+\dot{r}^2(z)\right)^{1/2}}\begin{pmatrix} r(z) & 0 \\ 0 & \ddot{r}(z) \end{pmatrix} \tag{22}$$

is obtained as the second fundamental form of a solid of revolution. With Eqs. (20) and (22), the Weingarten tensor of a solid of revolution reads as

$$\underline{\underline{\mathcal{W}}} = \begin{pmatrix} \frac{1}{r(z)\left[1+\dot{r}^2(z)\right]^{1/2}} & 0 \\ 0 & \frac{\ddot{r}(z)}{\left[1+\dot{r}^2(z)\right]^{3/2}} \end{pmatrix}. \tag{23}$$

The eigenvalues of this Weingarten tensor are its diagonal elements indicating the main curvatures κ_1 and κ_2. The main radii of curvature R_1 and R_2 are connected to the main curvatures κ_1 and κ_2 via

$$R_1 = \frac{1}{\kappa_1} = r(z)\left[1+\dot{r}^2(z)\right]^{1/2}, \tag{24a}$$

$$R_2 = \frac{1}{\kappa_2} = \frac{\left[1+\dot{r}^2(z)\right]^{3/2}}{\ddot{r}(z)}. \tag{24b}$$

With $\mathbf{\Omega} = (\vartheta, \varphi)$ denoting generalized polar coordinates and the mean radii of curvature $R_1(\mathbf{\Omega})$ and $R_2(\mathbf{\Omega})$, the integral mean radius of curvature $\tilde{R}_\mathrm{P}$ can be written as

$$\begin{aligned}\tilde{R}_\mathrm{P} &= \frac{1}{4\pi}\oiint_{4\pi}\frac{1}{2}\left[R_1(\mathbf{\Omega}) + R_2(\mathbf{\Omega})\right]\,d\mathbf{\Omega} \\ &= \frac{1}{4\pi}\int_0^{2\pi}\int_{-1}^{1}\frac{1}{2}\left[R_1(\vartheta,\varphi) + R_2(\vartheta,\varphi)\right]\,d\,\cos\vartheta\,d\,\varphi.\end{aligned} \tag{25}$$

The latter expression can be expanded as

$$\begin{aligned}\tilde{R}_\mathrm{P} = \frac{1}{4\pi}\int_0^{2\pi}\int_{-1}^{1}\frac{1}{2}&\frac{R_1(\vartheta,\varphi)+R_2(\vartheta,\varphi)}{R_1(\vartheta,\varphi)R_2(\vartheta,\varphi)} \\ &\times R_2(\vartheta,\varphi)d\cos\vartheta\,R_1(\vartheta,\varphi)d\varphi,\end{aligned} \tag{26}$$

where $d\,S = R_2(\vartheta,\varphi)\,d\cos\vartheta R_1(\vartheta,\varphi)\,d\varphi$ denotes the infinitesimal surface element. The remaining integrand

$$\frac{1}{2}\frac{R_1(\vartheta,\varphi)+R_2(\vartheta,\varphi)}{R_1(\vartheta,\varphi)\,R_2(\vartheta,\varphi)} = \bar{\kappa}(\vartheta,\varphi) \tag{27}$$

is the mean curvature at (ϑ,φ). Hereby, the integral mean radius of curvature $\tilde{R}_\mathrm{P}$ can be expressed as the surface integral over the mean curvature $\bar{\kappa}(\vartheta,\varphi)$,

$$\tilde{R}_\mathrm{P} = \frac{1}{4\pi}\iint_S \frac{1}{2}\left[\frac{1}{R_1(\vartheta,\varphi)}+\frac{1}{R_2(\vartheta,\varphi)}\right] d^2S. \tag{28}$$

In cylinder coordinates, we can write the infinitesimal surface element $dS = ds\; r(z)d\varphi$ with the radius $r(z)$ of the meridian curve, the infinitesimal azimuthal angle element $d\varphi$, and the infinitesimal curve length element ds of the meridian curve $r(z)$. With Eq. (11), the integral mean radius of curvature $\tilde{R}_\mathrm{P}$, Eq. (28), can be rewritten as

$$\tilde{R}_\mathrm{P} = \frac{1}{4\pi}\int_0^{2\pi}\int_{-\nu r_\mathrm{eq}}^{\nu r_\mathrm{eq}} \frac{1}{2}\left[\frac{1}{R_1(z)}+\frac{1}{R_2(z)}\right] \times r(z)\,d\varphi\left[1+\dot{r}^2(z)\right]^{1/2} dz, \tag{29}$$

where r_eq denotes the equatorial radius and ν denotes the aspect ratio of the considered geometric object. Using Eq. (24a) and performing the integration over the azimuthal angle φ, which yields a factor 2π, one finally obtains

$$\tilde{R}_\mathrm{P} = \frac{1}{4}\int_{-\nu r_\mathrm{eq}}^{\nu r_\mathrm{eq}} \left[1+\frac{R_1(z)}{R_2(z)}\right] dz \tag{30}$$

since the radii of curvature are independent of the azimuthal angle φ and depend only on the height z due to axial symmetry. For solids of revolution with an equatorial mirror plane with the parity $r(z) = r(-z)$, the integral radius of curvature can be written as

$$\tilde{R}_\mathrm{P} = \frac{1}{2}\int_0^{\nu r_\mathrm{eq}} \left[1+\frac{R_1(z)}{R_2(z)}\right] dz. \tag{31}$$

The precondition for the existence of the integrals (30) and (31) is the absence of singularities in the curvature, which would result in discontinuities in the meridian curve $r(z)$ and its derivatives $\dot{r}(z)$ and $\ddot{r}(z)$.

III. ANALYTICAL SECOND VIRIAL COEFFICIENTS FOR DIFFERENTLY SHAPED SOLIDS OF REVOLUTION

A. Geometric objects with continuous surface curvature

1. Ellipsoid

The meridian curve of an ellipsoid with the equatorial radius $r_\mathrm{eq}^{(\mathrm{ell})}$ and the aspect ratio $\nu^{(\mathrm{ell})}$ is

$$r^{(\mathrm{ell})}(z) = \left(r_\mathrm{eq}^{2,(\mathrm{ell})} - \frac{z^2}{\nu^{2,(\mathrm{ell})}}\right)^{1/2}. \tag{32}$$

The meridian curve and its derivatives,

$$\dot{r}^{(\mathrm{ell})}(z) = \frac{dr^{(\mathrm{ell})}(z)}{dz} = -\frac{z}{\nu^{(\mathrm{ell})}\left(\nu^{2,(\mathrm{ell})}r_\mathrm{eq}^{2,(\mathrm{ell})} - z^2\right)^{1/2}}, \tag{33a}$$

$$\ddot{r}^{(\mathrm{ell})}(z) = \frac{d^2r^{(\mathrm{ell})}(z)}{dz^2} = -\frac{\nu^{(\mathrm{ell})}r_\mathrm{eq}^{2,(\mathrm{ell})}}{\left(\nu^{2,(\mathrm{ell})}r_\mathrm{eq}^{2,(\mathrm{ell})} - z^2\right)^{3/2}}, \tag{33b}$$

are continuous on the entire surface, i.e., for $-\nu^{(\mathrm{ell})}r_\mathrm{eq}^{(\mathrm{ell})} \le z \le \nu^{(\mathrm{ell})}r_\mathrm{eq}^{(\mathrm{ell})}$. The volume of an ellipsoid of revolution is $V^{(\mathrm{ell})} = 4\pi\nu^{(\mathrm{ell})}r_\mathrm{eq}^{3,(\mathrm{ell})}/3$, and its surface is

$$S^{(\mathrm{ell})}(\nu^{(\mathrm{ell})}, r_\mathrm{eq}^{(\mathrm{ell})}) = \begin{cases} \dfrac{2\pi r_\mathrm{eq}^{2,(\mathrm{ell})}}{\left(\nu^{2,(\mathrm{ell})}-1\right)^{1/2}}\left[\nu^{2,(\mathrm{ell})}\arcsin\left(\dfrac{\left(\nu^{2,(\mathrm{ell})}-1\right)^{1/2}}{\nu^{(\mathrm{ell})}}\right)+\left(\nu^{2,(\mathrm{ell})}-1\right)^{1/2}\right] & \nu^{(\mathrm{ell})} \ge 1 \\ \dfrac{2\pi r_\mathrm{eq}^{2,(\mathrm{ell})}}{\left(1-\nu^{2,(\mathrm{ell})}\right)^{1/2}}\left[\nu^{2,(\mathrm{ell})}\ln\left(\dfrac{1+\left(1-\nu^{2,(\mathrm{ell})}\right)^{1/2}}{\nu^{(\mathrm{ell})}}\right)+\left(1-\nu^{2,(\mathrm{ell})}\right)^{1/2}\right] & \nu^{(\mathrm{ell})} \le 1 \end{cases} \tag{34}$$

for prolate ($\nu^{(\mathrm{ell})} \ge 1$) and oblate ($\nu^{(\mathrm{ell})} \le 1$) ellipsoids of revolution. In the limit of a sphere ($\nu^{(\mathrm{ell})} = 1$) with both branches of Eq. (34),

$$\lim_{\nu^{(\mathrm{ell})}\to 1^+} S^{(\mathrm{ell})}(\nu^{(\mathrm{ell})}, r_\mathrm{eq}^{(\mathrm{ell})}) = \lim_{\nu^{(\mathrm{ell})}\to 1^-} S^{(\mathrm{ell})}(\nu^{(\mathrm{ell})}, r_\mathrm{eq}^{(\mathrm{ell})}) = 4\pi r_\mathrm{eq}^{2,(\mathrm{ell})}, \tag{35}$$

as the surface of a sphere with the radius $r_\mathrm{eq}^{(\mathrm{ell})}$ is obtained. Also in the limit $\nu^{(\mathrm{ell})} \to 0^+$, as expected, the surface of an infinitely thin cylinder of radius $r_\mathrm{eq}^{(\mathrm{ell})}$,

$$\lim_{\nu^{(\mathrm{ell})}\to 0^+} S(\nu^{(\mathrm{ell})}, r_\mathrm{eq}^{(\mathrm{ell})}) = 2\pi r_\mathrm{eq}^{2,(\mathrm{ell})}, \tag{36}$$

results. Employing Eqs. (24), (32), and (33), an ellipsoid's radii of curvature can be written as

$$R_1^{(\mathrm{ell})} = \frac{\left(\nu^{4,(\mathrm{ell})}r_\mathrm{eq}^{2,(\mathrm{ell})} - \left(\nu^{2,(\mathrm{ell})}-1\right)z^2\right)^{1/2}}{\nu^{2,(\mathrm{ell})}}, \tag{37a}$$

$$R_2^{(\mathrm{ell})} = \frac{\left(\nu^{4,(\mathrm{ell})}r_\mathrm{eq}^{2,(\mathrm{ell})} - \left(\nu^{2,(\mathrm{ell})}-1\right)z^2\right)^{3/2}}{\nu^{4,(\mathrm{ell})}r_\mathrm{eq}^{2,(\mathrm{ell})}}. \tag{37b}$$

With Eq. (31), the mean radius of curvature of an ellipsoid of revolution reads as

$$\tilde{R}^{(\mathrm{ell})} = \int_0^{\nu^{(\mathrm{ell})} r_{\mathrm{eq}}^{(\mathrm{ell})}} \frac{1}{2}\left[1 + \frac{\nu^{2,(\mathrm{ell})} r_{\mathrm{eq}}^{2,(\mathrm{ell})}}{\nu^{4,(\mathrm{ell})} r_{\mathrm{eq}}^{2,(\mathrm{ell})} - \left(\nu^{2,(\mathrm{ell})} - 1\right) z^2}\right] dz \tag{38}$$

with the analytical result

$$\tilde{R}^{(\mathrm{ell})} = \begin{cases} \dfrac{\nu^{(\mathrm{ell})} r_{\mathrm{eq}}^{(\mathrm{ell})}}{2} + \dfrac{r_{\mathrm{eq}}^{(\mathrm{ell})}}{2\left(\nu^{2,(\mathrm{ell})} - 1\right)^{1/2}} \operatorname{arctanh}\left(\dfrac{\left(\nu^{2,(\mathrm{ell})} - 1\right)^{1/2}}{\nu^{(\mathrm{ell})}}\right) & \nu^{(\mathrm{ell})} \geq 1 \\ \dfrac{\nu^{(\mathrm{ell})} r_{\mathrm{eq}}^{(\mathrm{ell})}}{2} + \dfrac{r_{\mathrm{eq}}^{(\mathrm{ell})}}{2\left(1 - \nu^{2,(\mathrm{ell})}\right)^{1/2}} \arctan\left(\dfrac{\left(1 - \nu^{2,(\mathrm{ell})}\right)^{1/2}}{\nu^{(\mathrm{ell})}}\right) & \nu^{(\mathrm{ell})} \leq 1 \end{cases}. \tag{39}$$

For both branches of Eq. (39), the mean radius of a sphere with the equatorial radius $r_{\mathrm{eq}}^{(\mathrm{ell})}$,

$$\lim_{\nu^{(\mathrm{ell})} \to 1^-} \tilde{R}^{(\mathrm{ell})}(\nu^{(\mathrm{ell})}) = \lim_{\nu^{(\mathrm{ell})} \to 1^+} \tilde{R}^{(\mathrm{ell})}(\nu^{(\mathrm{ell})}) = r_{\mathrm{eq}}^{(\mathrm{ell})}, \tag{40}$$

is obtained in the limit $\nu^{(\mathrm{ell})} \to 1$. In the limit of an infinitely thin cylinder with $\nu^{(\mathrm{ell})} \to 0^+$, the limit

$$\lim_{\nu^{(\mathrm{ell})} \to 0^+} \tilde{R}^{(\mathrm{ell})}(\nu^{(\mathrm{ell})}) = \frac{\pi}{4} r_{\mathrm{eq}}^{(\mathrm{ell})} \tag{41}$$

is obtained, which is identical to the result of Isihara[12] for a cylinder derived in a different way.

With the volume, surface, and mean radius of curvature, the reduced second virial coefficient $B_2^{*,(\mathrm{ell})}(\nu^{(\mathrm{ell})}, r_{\mathrm{eq}}^{(\mathrm{ell})})$ of an ellipsoid is analytically obtained, both for prolate and oblate ellipsoids of revolution.

2. Spherocylinder

A second geometry without singularities in its surface curvature is a spherocylinder with the meridian curve

$$r^{(\mathrm{sc})}(z) = \begin{cases} \left[r_{\mathrm{eq}}^{2,(\mathrm{sc})} - \left(z - (\nu^{(\mathrm{sc})} - 1) r_{\mathrm{eq}}^{(\mathrm{sc})}\right)^2\right]^{1/2} & (\nu^{(\mathrm{sc})} - 1) r_{\mathrm{eq}}^{(\mathrm{sc})} < z \leq \nu^{(\mathrm{sc})} r_{\mathrm{eq}}^{(\mathrm{sc})} \\ r_{\mathrm{eq}}^{(\mathrm{sc})} & -(\nu^{(\mathrm{sc})} - 1) r_{\mathrm{eq}}^{(\mathrm{sc})} \leq z \leq (\nu^{(\mathrm{sc})} - 1) r_{\mathrm{eq}}^{(\mathrm{sc})} \\ \left[r_{\mathrm{eq}}^{2,(\mathrm{sc})} + \left(z - (\nu^{(\mathrm{sc})} - 1) r_{\mathrm{eq}}^{(\mathrm{sc})}\right)^2\right]^{1/2} & -\nu^{(\mathrm{sc})} r_{\mathrm{eq}}^{(\mathrm{sc})} \leq z < -(\nu^{(\mathrm{sc})} - 1) r_{\mathrm{eq}}^{(\mathrm{sc})} \end{cases}, \tag{42}$$

i.e., a cylinder of radius $r_{\mathrm{eq}}^{(\mathrm{sc})}$ and length $2(\nu^{(\mathrm{sc})} - 1) r_{\mathrm{eq}}^{(\mathrm{sc})}$ continued with two hemispheres of radius $r_{\mathrm{eq}}^{(\mathrm{sc})}$ at the top and bottom circle. Its volume is given by

$$V^{(\mathrm{sc})} = 2\pi r_{\mathrm{eq}}^{3,(\mathrm{sc})} \left(\nu^{(\mathrm{sc})} - \frac{1}{3}\right) \tag{43}$$

and its surface by

$$S^{(\mathrm{sc})} = 4\pi r_{\mathrm{eq}}^{2,(\mathrm{sc})} \nu^{(\mathrm{sc})}. \tag{44}$$

Employing Eq. (31), the mean radius of curvature $\tilde{R}^{(\mathrm{sc})}$ can easily be obtained from simple geometrical considerations. In the cylindrical part, one radius of curvature is $r_{\mathrm{eq}}^{(\mathrm{sc})}$, and the second one is infinite since the meridian curve is straight in this region. Within the hemispheres, both radii of curvature are identical, $R_1 = R_2 = r_{\mathrm{eq}}^{(\mathrm{sc})}$. Hence, $\tilde{R}^{(\mathrm{sc})}$ can be written as

$$\tilde{R}^{(\mathrm{sc})} = r_{\mathrm{eq}}^{(\mathrm{sc})} + \frac{1}{2}(\nu^{(\mathrm{sc})} - 1) r_{\mathrm{eq}}^{(\mathrm{sc})} = \frac{\nu^{(\mathrm{sc})} + 1}{2} r_{\mathrm{eq}}^{(\mathrm{sc})}. \tag{45}$$

In the limit $\nu^{(\mathrm{sc})} \to 1^+$, spherocylinder and ellipsoid of revolution approach a sphere with radius r_{eq}. For a sphere, the reduced second virial coefficient

$$B_2^{*,(\mathrm{sph})} = 1 + \frac{4\pi r_{\mathrm{eq}}^2 r_{\mathrm{eq}}}{\frac{4}{3}\pi r_{\mathrm{eq}}^3} = 4 \tag{46}$$

results, which already has been derived by van der Waals.

B. Second virial coefficients of bodies with singularities of their surface curvature

The calculation of the mean radius of curvature $\tilde{R}_{\mathrm{P}}$ with Eq. (31) needs particular care if the geometry contains singularities in its surface curvature. For convex solids of revolution, this occurs if the first derivative of the meridian curve $\dot{r}(z)$ is not continuous, e.g., in the case of a cylinder. These discontinuities, however, are removable for convex bodies of revolution.

1. Spindle

A spindle contains singularities of curvature at its apices. A spindle's meridional curve can with

$$\alpha = \frac{r_{\mathrm{eq}}^{(\mathrm{sp})}\left(1 + \nu^{2,(\mathrm{sp})}\right)}{2} \tag{47}$$

be written as

$$r^{(\mathrm{sp})}(z) = r_{\mathrm{eq}}^{(\mathrm{sp})} - \alpha + \left(\alpha^2 - z^2\right)^{1/2}. \tag{48}$$

In the limit $\nu^{(\mathrm{sp})} \to 1$, also a spindle approaches a sphere of radius $r_{\mathrm{eq}}^{(\mathrm{sp})}$. For aspect ratios $\nu^{(\mathrm{sp})} > 1$, however, apices at $z = \pm\nu^{(\mathrm{sp})} r_{\mathrm{eq}}^{(\mathrm{sp})}$ with $r(\pm\,\nu^{(\mathrm{sp})} r_{\mathrm{eq}}^{(\mathrm{sp})}) = 0$ exist. The derivatives of the meridian curve are

$$\dot{r}^{(\mathrm{sp})}(z) = -\frac{z}{\left(\alpha^2 - z^2\right)^{1/2}}, \tag{49a}$$

$$\ddot{r}^{(\mathrm{sp})}(z) = -\frac{\alpha^2}{\left(\alpha^2 - z^2\right)^{3/2}}, \tag{49b}$$

leading with Eqs. (24) to a spindle's radii of curvature

$$R_1^{(\mathrm{sp})} = \alpha\left[\frac{r_{\mathrm{eq}}^{(\mathrm{sp})} - \alpha}{\left(\alpha^2 - z^2\right)^{1/2}} + 1\right], \tag{50a}$$

$$R_2^{(\mathrm{sp})} = \alpha. \tag{50b}$$

The radius of curvature $R_2^{(\mathrm{sp})}$ does not depend on z since the meridian curve is an arc with radius α. Employing Eq. (12), the surface of a spindle reads as

$$S^{(\mathrm{sp})} = 2\pi r_{\mathrm{eq}}^{2,(\mathrm{sp})}\left[\nu^{(\mathrm{sp})}\left(\nu^{2,(\mathrm{sp})} + 1\right) + \frac{1 - \nu^{4,(\mathrm{sp})}}{2}\arcsin\left(\frac{2\nu^{(\mathrm{sp})}}{\nu^{2,(\mathrm{sp})} + 1}\right)\right], \tag{51}$$

and its volume[20] is

$$V^{(\mathrm{sp})} = \frac{\pi r_{\mathrm{eq}}^{3,(\mathrm{sp})}}{12}\left[6\nu^{5,(\mathrm{sp})} + 4\nu^{3,(\mathrm{sp})} + 6\nu^{(\mathrm{sp})} - 3\left(\nu^{6,(\mathrm{sp})} + \nu^{4,(\mathrm{sp})} - \nu^{2,(\mathrm{sp})} - 1\right) \times \arcsin\left(\frac{2\nu^{(\mathrm{sp})}}{\nu^{2,(\mathrm{sp})} + 1}\right)\right]. \tag{52}$$

Except both apices at $z = \pm\nu^{(\mathrm{sp})} r_{\mathrm{eq}}^{(\mathrm{sp})}$, the principal radii of curvature are continuous. In the limits $-\nu^{(\mathrm{sp})} r_{\mathrm{eq}}^{(\mathrm{sp})} + \varepsilon < z < \nu^{(\mathrm{sp})} r_{\mathrm{eq}}^{(\mathrm{sp})} - \varepsilon$, employing Eq. (31), the mean radius of curvature is

$$\begin{aligned}\tilde{R}'^{(\mathrm{sp})}(\varepsilon) &= \frac{1}{2}\int_0^{\nu^{(\mathrm{sp})} r_{\mathrm{eq}}^{(\mathrm{sp})} - \varepsilon}\left[2 + \frac{r_{\mathrm{eq}}^{(\mathrm{sp})} - \alpha}{\left(\alpha^2 - z^2\right)^{1/2}}\right] dz \\ &= \nu^{(\mathrm{sp})} r_{\mathrm{eq}}^{(\mathrm{sp})} - \varepsilon - \frac{r_{\mathrm{eq}}^{(\mathrm{sp})}\left(\nu^{2,(\mathrm{sp})} - 1\right)}{4} \\ &\quad \times \arcsin\left[\frac{2\left(\nu^{(\mathrm{sp})} r_{\mathrm{eq}}^{(\mathrm{sp})} + \varepsilon\right)}{r_{\mathrm{eq}}^{(\mathrm{sp})}\left(\nu^{2,(\mathrm{sp})} + 1\right)}\right].\end{aligned} \tag{53}$$

The contribution of the singularity can be obtained by replacing the spindle's meridional curve in the limits $\nu^{(\mathrm{sp})} r_{\mathrm{eq}}^{(\mathrm{sp})} - \varepsilon < z < \nu^{(\mathrm{sp})} r_{\mathrm{eq}}^{(\mathrm{sp})}$ by the meridian curve of a sphere with

$$r^{(\mathrm{sp})}(\nu^{(\mathrm{sp})} r_{\mathrm{eq}}^{(\mathrm{sp})} - \varepsilon) = r^{(\mathrm{sph})}(\nu^{(\mathrm{sp})} r_{\mathrm{eq}}^{(\mathrm{sp})} - \varepsilon) \tag{54}$$

and

$$\dot{r}^{(\mathrm{sp})}(\nu^{(\mathrm{sp})} r_{\mathrm{eq}}^{(\mathrm{sp})} - \varepsilon) = \dot{r}^{(\mathrm{sph})}(\nu^{(\mathrm{sp})} r_{\mathrm{eq}}^{(\mathrm{sp})} - \varepsilon), \tag{55}$$

resulting in a continuous meridian curve and a continuous first derivative of the meridian curve at $z = \nu^{(\mathrm{sp})} r_{\mathrm{eq}}^{(\mathrm{sp})} - \varepsilon$ (Fig. 1). For convenience, a sphere with equatorial radius $r_{\mathrm{eq}}^{(\mathrm{sph})}$ centered at z_0 is used to continuously complete the spindle shape in the limit $\varepsilon \to 0$. The sphere's meridional curve reads as

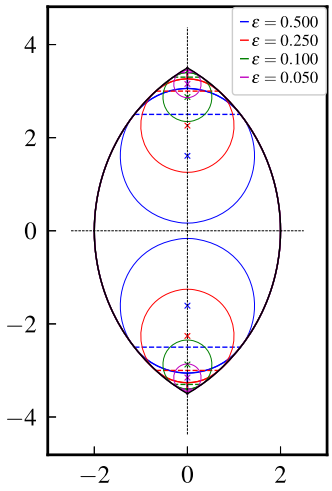

FIG. 1. Removing the singularities of surface curvature at a spindle's apices. Within the distance ε to each apex, the meridional curve of the spindle is replaced by that of a sphere ensuring continuity of the meridian curve and its first derivative in the distance ε to each apex. The crosses indicate the centers of spheres located at $z_0(\varepsilon)$.

$$r^{(\mathrm{sph})}(z, \varepsilon) = \left[r_{\mathrm{eq}}^{2,(\mathrm{sph})}(\varepsilon) - (z - z_0(\varepsilon))^2\right]^{1/2}, \tag{56}$$

with the parameters $r_{\mathrm{eq}}^{(\mathrm{sph})}(\varepsilon)$ and $z_0(\varepsilon)$ given in Eqs. (A1) and (A2). Since both radii of curvature of the sphere are identical, its main radius of curvature $\tilde{R}''^{(\mathrm{sp})}$ above $\nu^{(\mathrm{sp})} r_{\mathrm{eq}}^{(\mathrm{sp})} - \varepsilon$ reads, using Eq. (30), as

$$\tilde{R}''^{(\mathrm{sp})} = \frac{1}{2}\left[r_{\mathrm{eq}}^{(\mathrm{sph})} - \left(\nu^{(\mathrm{sp})} r_{\mathrm{eq}}^{(\mathrm{sp})} - \varepsilon - z_0\right)\right]. \tag{57}$$

In the limit $\varepsilon \to 0$, when the geometry approaches a spindle, with Eqs. (A3) and (A4),

$$\lim_{\varepsilon \to 0} \tilde{R}''^{(\mathrm{sp})} = 0 \tag{58}$$

results. Thus, the contribution of apices to the mean radius of curvature is $\tilde{R}''^{(\mathrm{sph})} = \tilde{R}''^{(\mathrm{sp})} = 0$, and the mean radius of curvature of a spindle can be written as

$$\begin{aligned}\tilde{R}^{(\mathrm{sp})} &= \lim_{\varepsilon \to 0}\left[\tilde{R}'^{(\mathrm{sp})}(\varepsilon) + \tilde{R}''^{(\mathrm{sp})}(\varepsilon)\right] \\ &= r_{\mathrm{eq}}^{(\mathrm{sp})}\left[\nu^{(\mathrm{sp})} - \frac{\nu^{2,(\mathrm{sp})} - 1}{4}\arcsin\left(\frac{2\nu^{(\mathrm{sp})}}{\nu^{2,(\mathrm{sp})} + 1}\right)\right].\end{aligned} \tag{59}$$

Since the curvature discontinuity of any geometry with apical singularities can be removed using segments of a sphere with vanishing radius, apical singularities do not contribute to the mean radius of curvature.

2. Lens

Unlike a spindle with two one-dimensional singularities at its apices, a lens has a two-dimensional singularity in its equatorial plane. A lens as an oblate solid of revolution with $\nu^{(\mathrm{lens})} \leq 1$ and the equatorial radius $r_{\mathrm{eq}}^{(\mathrm{lens})}$ is composed of two segments of a sphere (Fig. 2) with radius

$$R_0 = r_{\mathrm{eq}}^{(\mathrm{lens})}\frac{1 + \nu^{2,(\mathrm{lens})}}{2\nu^{(\mathrm{lens})}}. \tag{60}$$

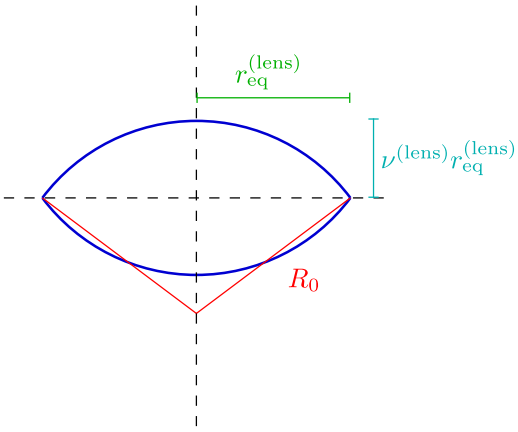

FIG. 2. Section of a lens as a solid of revolution composed of two sphere segments with sphere radius R_0 connected to the equatorial radius $r_{\mathrm{eq}}^{(\mathrm{lens})}$ and its aspect ratio $\nu^{(\mathrm{lens})}$.

In the limit $\nu^{(\mathrm{lens})} \to 1$, a lens approaches a sphere. Its meridional curve can be written as

$$r^{(\mathrm{lens})}(z) = \left(\frac{|z| r_{\mathrm{eq}}^{(\mathrm{lens})} (\nu^{2,(\mathrm{lens})} - 1) + \nu^{(\mathrm{lens})} (r_{\mathrm{eq}}^{2,(\mathrm{lens})} - z^2)}{\nu^{(\mathrm{lens})}} \right)^{1/2}. \tag{61}$$

The lens' volume is given by

$$V^{(\mathrm{lens})} = \pi r_{\mathrm{eq}}^{3,(\mathrm{lens})} \left(\nu^{(\mathrm{lens})} + \frac{\nu^{3,(\mathrm{lens})}}{3} \right) \tag{62}$$

and its surface by

$$S^{(\mathrm{lens})} = 2\pi r_{\mathrm{eq}}^{2,(\mathrm{lens})} \left(1 + \nu^{2,(\mathrm{lens})} \right). \tag{63}$$

The first derivative of the meridian curve, which is negative due to $\nu \leq 1$ for $z > 0$, reads as

$$\begin{aligned} \dot{r}^{(\mathrm{lens})}(z) &= \frac{dr^{(\mathrm{lens})}(z)}{dz} \\ &= \frac{r_{\mathrm{eq}}^{(\mathrm{lens})} (\nu^{2,(\mathrm{lens})} - 1) - 2\nu^{2,(\mathrm{lens})} z}{2\nu^{(\mathrm{lens})} r^{(\mathrm{lens})}(z)}. \end{aligned} \tag{64a}$$

The second derivative, which is negative due to the concave down curvature in the upper sphere segment, can be written as

$$\begin{aligned} \ddot{r}^{(\mathrm{lens})}(z) &= \frac{d^2 r^{(\mathrm{lens})}(z)}{dz^2} = -\frac{1}{4} \frac{r_{\mathrm{eq}}^{2,(\mathrm{lens})} \left(\nu^{2,(\mathrm{lens})} + 1 \right)^2}{\nu^{2,(\mathrm{lens})} r^{3,(\mathrm{lens})}(z)} \\ &= -\frac{R_0^2}{r^{3,(\mathrm{lens})}(z)}. \end{aligned} \tag{64b}$$

Using

$$\begin{aligned} \left[1 + \left(\frac{dr^{(\mathrm{lens})}(z)}{dz} \right)^2 \right]^{1/2} &= \pm \frac{1}{2} \frac{r_{\mathrm{eq}}^{(\mathrm{lens})} \left(\nu^{2,(\mathrm{lens})} + 1 \right)}{\nu^{(\mathrm{lens})} r^{(\mathrm{lens})}(z)} \\ &= \pm \frac{R_0}{r^{(\mathrm{lens})}(z)}, \end{aligned} \tag{65}$$

we can easily calculate the principal radii of curvature,

$$R_1^{(\mathrm{lens})} = r^{(\mathrm{lens})}(z) \left[1 + \left(\frac{dr^{(\mathrm{lens})}(z)}{dz} \right)^2 \right]^{1/2} = R_0, \tag{66a}$$

$$R_2^{(\mathrm{lens})} = \frac{-\left[1 + \left(\frac{dr^{(\mathrm{lens})}(z)}{dz} \right)^2 \right]^{3/2}}{\frac{d^2 r^{(\mathrm{lens})}(z)}{dz^2}} = \frac{-\frac{R_0^3}{r^{3,(\mathrm{lens})}(z)}}{-\frac{R_0^2}{r^{3,(\mathrm{lens})}(z)}} = R_0, \tag{66b}$$

which must of course be identical R_0. The integral mean radius of curvature except the singularity at $z = 0$ is

$$\tilde{R}'^{(\mathrm{lens})} = \int_{\varepsilon}^{\nu^{(\mathrm{lens})} r_{\mathrm{eq}}^{(\mathrm{lens})}} \frac{1}{2} \left(1 + \frac{R_1^{(\mathrm{lens})}}{R_2^{(\mathrm{lens})}} \right) dz = \nu^{(\mathrm{lens})} r_{\mathrm{eq}}^{(\mathrm{lens})} - \varepsilon. \tag{67}$$

To calculate the contribution of the singularity, which disappears in the limit of a sphere with $\nu^{(\mathrm{lens})} = 1$, we approximate a lens in the limits $-\varepsilon < z < \varepsilon$ by an oblate ellipsoid with the equatorial diameter $r_{\mathrm{eq}}^{(\mathrm{ell})}(\varepsilon)$ and the aspect ratio $\nu^{(\mathrm{ell})}(\varepsilon)$ such that

$$r^{(\mathrm{lens})}(\pm\varepsilon) = r^{(\mathrm{ell})}(\pm\varepsilon) \tag{68a}$$

and

$$\dot{r}^{(\mathrm{lens})}(\pm\varepsilon) = \dot{r}^{(\mathrm{ell})}(\pm\varepsilon), \tag{68b}$$

i.e., the meridian curve and its first derivative are continuous (Fig. 3). The contribution to the mean radius of curvature originating from the singularity in the equatorial plane can with Eqs. (30), (37a), and (37b) be expressed as

$$\tilde{R}''^{(\mathrm{lens})} = \int_{-\epsilon}^{\epsilon} \frac{1}{4} \left[1 + \frac{\nu^{2,(\mathrm{ell})} r_{\mathrm{eq}}^{2,(\mathrm{ell})}}{\nu^{4,(\mathrm{ell})} r_{\mathrm{eq}}^{2,(\mathrm{ell})} - \left(\nu^{2,(\mathrm{ell})} - 1 \right) z^2} \right] dz. \tag{69}$$

Using Eqs. (B1) and (B2), the latter integral can be solved analytically [cf. Eq. (39)]. With Eq. (B5), a lens' mean radius

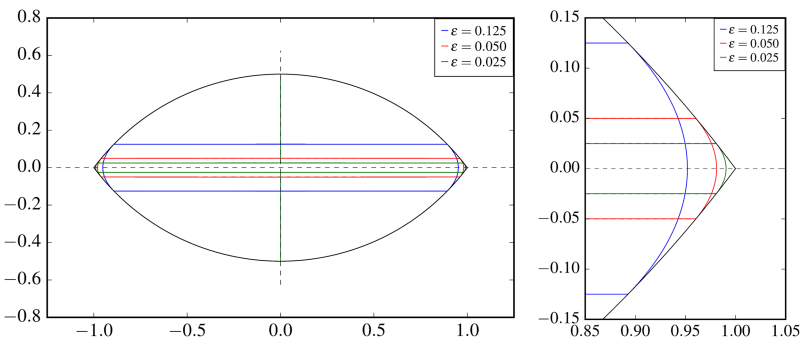

FIG. 3. Continuous completion of a cut-out lens by an ellipsoid. The continuity of the meridian curve and its first derivative can be seen in the magnified section on the right-hand side. The contribution of the equatorial singularity to the mean radius of curvature is obtained in the limit $\varepsilon \to 0$ with an infinitely thin ellipsoid with $r_{\mathrm{eq}}^{(\mathrm{ell})} = r_{\mathrm{eq}}^{(\mathrm{lens})}$.

of curvature in the limit $\varepsilon \to 0$ can be written as

$$\tilde{R}^{(\mathrm{lens})} = \lim_{\varepsilon\to 0}\left[\tilde{R}'^{(\mathrm{lens})}(\varepsilon) + \tilde{R}''^{(\mathrm{lens})}(\varepsilon)\right] = r_{\mathrm{eq}}^{(\mathrm{lens})}\left[\nu^{(\mathrm{lens})} + \frac{1}{2}\arctan\left(\frac{1-\nu^{2,(\mathrm{lens})}}{2\nu^{(\mathrm{lens})}}\right)\right]. \quad (70)$$

In the limit $\nu^{(\mathrm{lens})} \to 1$, as expected, the mean radius of curvature $\tilde{R}^{(\mathrm{lens})} = r_{\mathrm{eq}}^{(\mathrm{sph})}$ of a sphere with radius $r_{\mathrm{eq}}^{(\mathrm{sph})}$ results, while in the limit $\nu^{(\mathrm{lens})} \to 0^+$, an infinitely thin cylinder's mean radius of curvature $\tilde{R}^{(\mathrm{lens})} = \pi r_{\mathrm{eq}}^{(\mathrm{lens})}/4$ is obtained. Note that

$$\tan\xi = \lim_{z\to 0^+}\left|\frac{dr^{(\mathrm{lens})}(z)}{dz}\right| = \frac{1-\nu^{2,(\mathrm{lens})}}{2\nu^{(\mathrm{lens})}} \quad (71)$$

is the tangent of the angle enclosed between the z-direction and the first derivative of the meridian curve $\dot{r}^{(\mathrm{lens})}$ $(z \to 0^+)$ (Fig. 4). As a consequence, the angle between the meridian curves' tangents at $z \to 0^+$ and $z \to 0^-$ is $\zeta = \pi - 2\xi$. Using Eq. (70), the contribution of the singularity at $z = 0$ with radius $r^{(\mathrm{lens})}(0) = r_{\mathrm{eq}}^{(\mathrm{lens})}$ can be written as

$$\tilde{R}''^{(\mathrm{lens})} = \frac{r_{\mathrm{eq}}^{(\mathrm{lens})}}{2}\xi = \frac{r_{\mathrm{eq}}^{(\mathrm{lens})}}{4}(\pi - \zeta). \quad (72)$$

3. Double cone

Similar to a lens, also a double cone, which exists both as a prolate and oblate solid of revolution, possesses a two-dimensional singularity of surface curvature at its equator in addition to one-dimensional singularities at its apices. In the same manner as already shown for a spindle, a truncated double cone can be continuously completed by spheres with vanishing radii close to an apex, whose contribution to the mean radius of curvature vanishes, too.

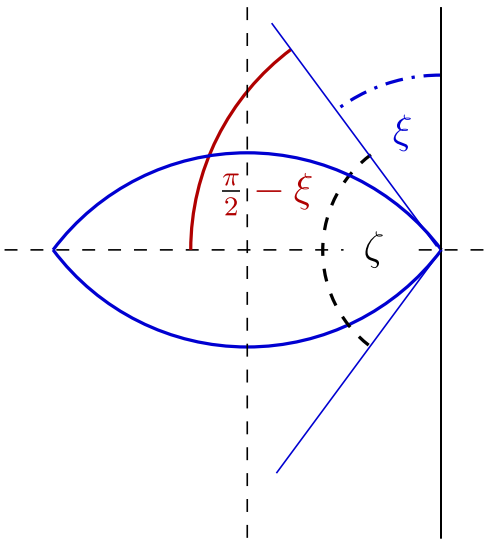

FIG. 4. The contribution of a lens' singularity in its surface curvature can be expressed by the angle ζ enclosed between the meridian curve's tangents at $z \to 0^+$ and $z \to 0^-$ and the equatorial radius $r^{(\mathrm{lens})}(0) = r_{\mathrm{eq}}^{(\mathrm{lens})}$. In the limit of a sphere, with $\zeta = \pi$, the singularity disappears and with $\tilde{R}''^{(\mathrm{lens})} = 0$ does not contribute to the mean radius of curvature. In contrast, with $\zeta = 0$, in the limit of an infinitely thin lens, $\tilde{R}''^{(\mathrm{lens})} = \pi r_{\mathrm{eq}}^{(\mathrm{lens})}/4$ is the only contribution to the mean radius of curvature.

The surface and volume of a double cone are

$$S^{(\mathrm{dc})} = 2\pi\left(1+\nu^{2,(\mathrm{dc})}\right)^{1/2} r_{\mathrm{eq}}^{2,(\mathrm{dc})} \quad (73)$$

and

$$V^{(\mathrm{dc})} = \frac{2}{3}\pi\nu^{(\mathrm{dc})} r_{\mathrm{eq}}^{3,(\mathrm{dc})}. \quad (74)$$

Let us analyze in analogy to a lens the contribution of the two-dimensional singularity to the mean radius of curvature by a continuous completion of a cut-out double cone. Details are deposited in the supplementary material (Sec. S-I). Since the meridian curve of a double cone is straight, the principal radius of curvature $R_2^{(\mathrm{dc})}$ is infinite. Thus, except the singularity, we obtain with Eq. (31)

$$\tilde{R}'^{(\mathrm{dc})} = \frac{1}{2}\int_0^{\nu^{(\mathrm{dc})} r_{\mathrm{eq}}^{(\mathrm{dc})}} dz = \frac{\nu^{(\mathrm{dc})} r_{\mathrm{eq}}^{(\mathrm{dc})}}{2} \quad (75)$$

as mean radius of curvature. A double cone encloses at its equatorial singularity with radius $r_{\mathrm{eq}}^{(\mathrm{dc})}$ the angle $\xi = \arctan(\nu^{-1})$ with the z-direction. Hence the contribution of this singularity to the mean radius of curvature is

$$\tilde{R}'' = \frac{r_{\mathrm{eq}}^{(\mathrm{dc})}}{2}\arctan\left(\frac{1}{\nu^{(\mathrm{dc})}}\right). \quad (76)$$

As a consequence, a double cone's mean radius of curvature can be written as[35]

$$\tilde{R}^{(\mathrm{dc})} = \frac{\nu^{(\mathrm{dc})} r_{\mathrm{eq}}^{(\mathrm{dc})}}{2} + \frac{r_{\mathrm{eq}}^{(\mathrm{dc})}}{2}\arctan\left(\frac{1}{\nu^{(\mathrm{dc})}}\right). \quad (77)$$

Just as in the case of a lens, a double cone approaches an infinitely thin plate in the limit $\nu^{(\mathrm{dc})} \to 0$ with the expected mean radius of curvature

$$\tilde{R}^{(\mathrm{dc})} = \lim_{\nu^{(\mathrm{dc})}\to 0^+}\left[\frac{\nu^{(\mathrm{dc})} r_{\mathrm{eq}}^{(\mathrm{dc})}}{2} + \frac{r_{\mathrm{eq}}^{(\mathrm{dc})}}{2}\arctan\left(\frac{1}{\nu^{(\mathrm{dc})}}\right)\right] = \frac{\pi r_{\mathrm{eq}}^{(\mathrm{dc})}}{4}. \quad (78)$$

In contrast, for $\nu^{(\mathrm{dc})} \to \infty$, the singularity in the equatorial plane disappears and the mean radius of curvature approaches that of an infinitely long cylinder.

C. Cylinder

A cylinder with the meridian curve

$$r^{(\mathrm{cyl})}(z) = r_{\mathrm{eq}}^{(\mathrm{cyl})} \quad (79)$$

possesses two singularities of surface curvature at $z = \pm\nu^{(\mathrm{cyl})} r_{\mathrm{eq}}^{(\mathrm{cyl})}$. A cylinder can easily be completed continuously by the upper half of an ellipsoid at the top face and the lower half of an ellipsoid at its bottom face. The equatorial radii of the half-ellipsoids equal the cylinder radius with $r_{\mathrm{eq}}^{(\mathrm{ell})} = r_{\mathrm{eq}}^{(\mathrm{cyl})}$. The volume of a cylinder with an aspect ratio $\nu^{(\mathrm{cyl})}$ is

$$V^{(\mathrm{cyl})} = 2\pi r_{\mathrm{eq}}^{3,(\mathrm{cyl})}\nu^{(\mathrm{cyl})}, \quad (80)$$

and its surface is

$$S^{(\mathrm{cyl})} = 2\pi r_{\mathrm{eq}}^{2,(\mathrm{cyl})}\left(1+2\nu^{(\mathrm{cyl})}\right). \quad (81)$$

Similar to the double cone, the meridian curve of the cylinder is straight and both derivatives $\dot{r}^{(\mathrm{cyl})}(z) = 0$ and $\ddot{r}^{(\mathrm{cyl})}(z) = 0$ vanish. Hence, the principal radii of curvature are $R_1^{(\mathrm{cyl})} = r_{\mathrm{eq}}^{(\mathrm{cyl})}$ and $R_2^{(\mathrm{cyl})} = \infty$.

Except the singularities at $z = \pm\nu^{(\mathrm{cyl})} r_{\mathrm{eq}}^{(\mathrm{cyl})}$, a cylinder's mean radius of curvature is according to Eq. (31)

$$\tilde{R}'^{(\mathrm{cyl})} = \frac{1}{2} \int_{-\nu^{(\mathrm{cyl})} r_{\mathrm{eq}}^{(\mathrm{cyl})} + \varepsilon}^{\nu^{(\mathrm{cyl})} r_{\mathrm{eq}}^{(\mathrm{cyl})} - \varepsilon} dz = \frac{\nu^{(\mathrm{cyl})} r_{\mathrm{eq}}^{(\mathrm{cyl})}}{2} (1 - \varepsilon). \tag{82}$$

In the limit $\nu^{(\mathrm{cyl})} \to 0^+$, employing Eq. (41), a contribution $\tilde{R}''^{(\mathrm{cyl})} = \pi r_{\mathrm{eq}}^{(\mathrm{cyl})}/8$ results from each circular singularity, independent of the cylinder's aspect ratio. Hence, the total mean radius of curvature of a cylinder can be written as

$$\tilde{R}^{(\mathrm{cyl})} = r_{\mathrm{eq}}^{(\mathrm{cyl})} \left(\frac{\nu^{(\mathrm{cyl})}}{2} + \frac{\pi}{4} \right). \tag{83}$$

Also in the case of a cylinder, the contribution of both singularities can be expressed using the moduli $|dr^{(\mathrm{cyl})}(z)/dz| = \infty$ at $z \to \left(\nu^{(\mathrm{cyl})} r_{\mathrm{eq}}^{(\mathrm{cyl})}\right)^+$ and $z \to \left(\nu^{(\mathrm{cyl})} r_{\mathrm{eq}}^{(\mathrm{cyl})}\right)^-$. For both singularities together, with $\xi = \pi/2$, the contribution $\tilde{R}'' = \pi r_{\mathrm{eq}}^{(\mathrm{cyl})}/4$ to the mean radius of curvature results.

IV. RESULTS

A. Prolate geometries

Employing methods of differential geometry, second virial coefficients of arbitrarily shaped, convex hard solids of revolution are analytically accessible. Let us first compare different prolate geometries (Fig. 5).

Since the geometric measures V_{P}, S_{P}, and $\tilde{R}_{\mathrm{P}}$ in the limit $\nu \to \infty$ have contributions proportional to ν, in the limit of infinite aspect ratio, a proportionality $B(\nu) \propto \nu^2$ results for the second virial coefficient (Fig. 6). As a consequence, constant ratios of the second virial coefficients exist in the limit $\nu \to \infty$. At an infinite aspect ratio, we obtain the ratios

$$\lim_{\nu\to\infty} \frac{B_2^{(\mathrm{cyl})}(\nu)}{B_2^{(\mathrm{ell})}(\nu)} = \frac{4}{\pi}, \tag{84a}$$

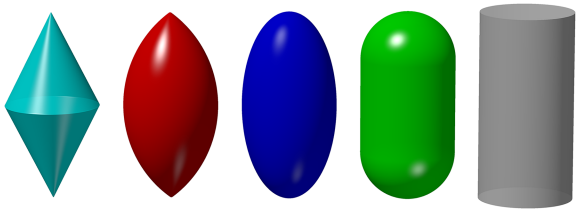

FIG. 5. Prolate solids of revolution with an aspect ratio $\nu = 2$. From left to right, a double cone, a spindle, an ellipsoid, a spherocylinder, and a cylinder are displayed. All shapes to the left of any geometry are strict subsets of their right neighbors. The spindle, the ellipsoid, and the spherocylinder approach in the limit $\nu = 1$ a sphere. While spindles and spherocylinders exist only for aspect ratios $\nu \geq 1$, oblate analogs of double cones, ellipsoids, and cylinders with $\nu < 1$ exist.

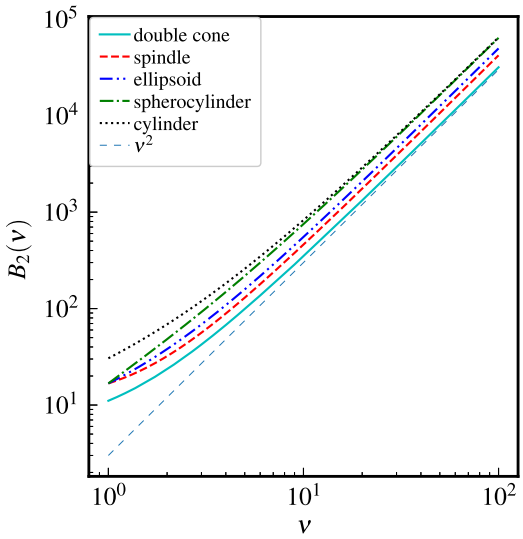

FIG. 6. Second virial coefficients for prolate solids of revolution with $r_{\mathrm{eq}} = 1$. Since in the limit $\nu \to \infty$ the geometric measures V_{P}, S_{P}, and $\tilde{R}_{\mathrm{P}}$ are proportional to the aspect ratio, a proportionality $B_2(\nu) \propto \nu^2$ results for an infinite aspect ratio. The thin dashed line represents ν^2 as a guide to the eye.

$$\lim_{\nu\to\infty} \frac{B_2^{(\mathrm{sc})}(\nu)}{B_2^{(\mathrm{ell})}(\nu)} = \frac{4}{\pi}, \tag{84b}$$

$$\lim_{\nu\to\infty} \frac{B_2^{(\mathrm{sp})}(\nu)}{B_2^{(\mathrm{ell})}(\nu)} = \frac{8}{3\pi}, \tag{84c}$$

$$\lim_{\nu\to\infty} \frac{B_2^{(\mathrm{dc})}(\nu)}{B_2^{(\mathrm{ell})}(\nu)} = \frac{2}{\pi} \tag{84d}$$

for different shapes. As expected, for $\nu \to \infty$, the difference between a spherocylinder and a cylinder vanishes. With increasing volume, the second virial coefficients as mutual excluded volume increase, too, in the order $B_2^{(\mathrm{dc})}(\infty) < B_2^{(\mathrm{sp})}(\infty) < B_2^{(\mathrm{ell})}(\infty) < B_2^{(\mathrm{sc})}(\infty) = B_2^{(\mathrm{cyl})}(\infty)$.

A useful measure for the mutual excluded volume related to a particle's volume is the reduced second virial coefficient B_2^* as given in Eq. (7). Normalization of virial coefficients B_n of order n to powers $n - 1$ of the particle volume leads to a representation of the virial series in powers of the volume fraction $\varphi = \varrho V_{\mathrm{P}}$,

$$\begin{aligned} \frac{p}{k_{\mathrm{B}}T} &= \varrho \left[1 + \frac{B_2}{V_{\mathrm{P}}}\varphi + \frac{B_3}{V_{\mathrm{P}}^2}\varphi^2 + \frac{B_4}{V_{\mathrm{P}}^3}\varphi^3 + \cdots \right] \\ &= \varrho \left[1 + \sum_{n=2}^{\infty} B_n^* \varphi^{n-1} \right], \end{aligned} \tag{85}$$

with $B_n^* = B_n / V_{\mathrm{P}}^{n-1}$.

Hence, a comparison of the reduced second virial coefficients can give insights into the mutual excluded volume in dependence on the aspect ratio at identical volume fraction of differently shaped particles.

In the limit $\nu \to \infty$, the proportionality $B_2^* \propto \nu$ is obtained for the reduced second virial coefficients, whose ratios are

$$\lim_{\nu\to\infty} \frac{B_2^{*,(\mathrm{cyl})}(\nu)}{B_2^{*,(\mathrm{ell})}(\nu)} = \frac{8}{3\pi}, \tag{86a}$$

$$\lim_{\nu\to\infty} \frac{B_2^{*,(\mathrm{sc})}(\nu)}{B_2^{*,(\mathrm{ell})}(\nu)} = \frac{8}{3\pi}, \tag{86b}$$

$$\lim_{\nu\to\infty} \frac{B_2^{*,(\mathrm{sp})}(\nu)}{B_2^{*,(\mathrm{ell})}(\nu)} = \frac{10}{3\pi}, \tag{86c}$$

$$\lim_{\nu\to\infty} \frac{B_2^{*,(\mathrm{dc})}(\nu)}{B_2^{*,(\mathrm{ell})}(\nu)} = \frac{4}{\pi}. \tag{86d}$$

Normalized to the particle volume, with $B_2^{*,(\mathrm{dc})}(\infty) > B_2^{*,(\mathrm{sp})}(\infty) > B_2^{*,(\mathrm{sc})}(\infty) = B_2^{*,(\mathrm{cyl})}(\infty)$, a decreasing series of reduced second virial coefficients with increasing particle volume from double cone to cylinder results.

Since ellipsoid, spindle, and spherocylinder approach a sphere at the aspect ratio $\nu = 1$, the reduced second virial coefficients for these geometries are identical, $B_2^{*,(\mathrm{ell})}(1) = B_2^{*,(\mathrm{sp})}(1) = B_2^{*,(\mathrm{sc})}(1) = 4$ (Fig. 7). With increasing aspect ratio, the reduced second virial coefficient of a spindle initially decreases compared to an ellipsoid, while that of a spherocylinder initially increases relative to an ellipsoid. The minimum $B_2^{*,(\mathrm{sp})}/B_2^{*,(\mathrm{ell})} = 0.988\,183\,2$ is reached at the aspect ratio $\nu = 2.048\,213$. For $\nu > 3.539\,816$, the reduced second virial coefficient of a spindle exceeds that of an ellipsoid. In contrast, the reduced second virial coefficient of a spherocylinder initially increases with increasing aspect ratio, approaching a maximum at $\nu = 2.143\,270$ with $B_2^{*,(\mathrm{sc})}/B_2^{*,(\mathrm{ell})} = 1.013\,773$. For $\nu > 3.718\,983$, the reduced second virial coefficient of a spherocylinder is smaller than that of an ellipsoid (Fig. 8). Also the reduced second virial coefficient of a cylinder becomes for $\nu > 9.731\,169$ smaller than that of an ellipsoid and asymptotically approaches that of a spherocylinder for $\nu \to \infty$.

The maximum ratio of a cylinder's reduced second virial coefficient to that of an ellipsoid with $B_2^{*,(\mathrm{cyl})}/B_2^{*,(\mathrm{ell})} = 1.221\,161$ occurs for slightly prolate cylinders with the aspect ratio $\nu = 1.303\,961$. The minimum ratio of a double cone's reduced second virial coefficient to that of an ellipsoid occurs at $\nu = 1.971\,481$ with the ratio $B_2^{*,(\mathrm{dc})}/B_2^{*,(\mathrm{ell})} = 1.130\,676$. The reduced second virial coefficient of a double cone exceeds that of a cylinder for $\nu > 3.231\,733$, while that of a spindle exceeds that of a cylinder for $\nu > 7.617\,511$. The characteristic aspect ratios and related second virial coefficients given in this section are obtained numerically with an arbitrary precision algorithm and rounded to six decimal places since analytical expressions for ν could not be obtained.

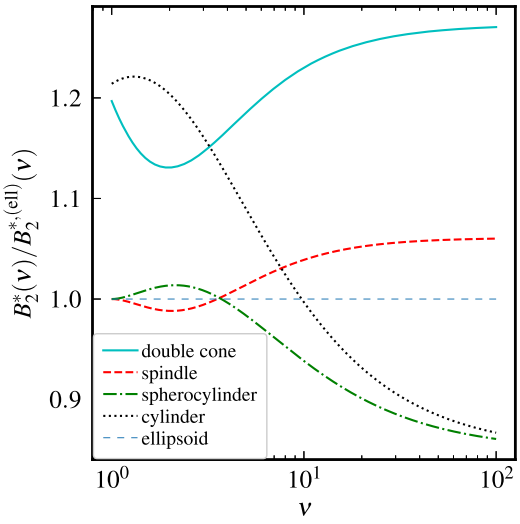

FIG. 7. Reduced second virial coefficients $B_2^*(\nu)$ for different solids of revolution with equatorial radius $r_{\mathrm{eq}} = 1$ normalized to the reduced second virial coefficient of ellipsoids $B_2^{*,(\mathrm{ell})}(\nu)$.

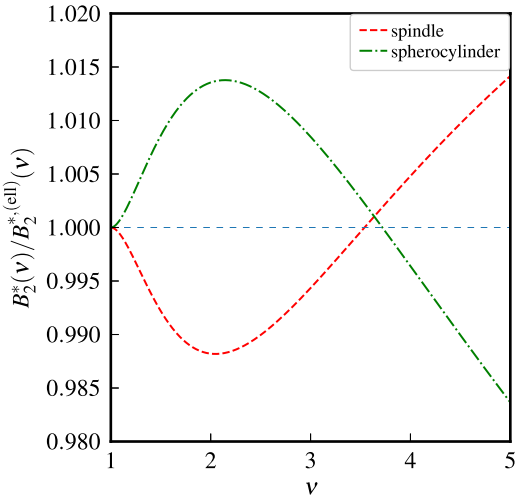

FIG. 8. Reduced second virial coefficients $B_2^*(\nu)$ for spindles, ellipsoids, and spherocylinders with equatorial radius $r_{\mathrm{eq}} = 1$ normalized to the reduced second virial coefficient of ellipsoids $B_2^{*,(\mathrm{ell})}(\nu)$.

B. Oblate geometries

As oblate geometries, double cones, lenses, ellipsoids, and cylinders (Fig. 9) are compared. For $\nu = 1$, lenses and ellipsoids are spheres. All geometries except lenses also exist as prolate solids. Again, double cones are strict subsets of all other geometries, lenses of ellipsoids and cylinders, and, finally, ellipsoids of cylinders.

In the limit $\nu \to 0$, all solids of revolution approach an infinitely thin circular plate, resulting in identical second virial coefficients,

$$\lim_{\nu\to 0^+} B_2^{(\mathrm{dc})}(\nu) = \lim_{\nu\to 0^+} B_2^{(\mathrm{lens})}(\nu) = \lim_{\nu\to 0^+} B_2^{(\mathrm{ell})}(\nu) = \lim_{\nu\to 0^+} B_2^{(\mathrm{cyl})}(\nu) = \frac{\pi^2 r_{\mathrm{eq}}^3}{2}, \tag{87}$$

as displayed in Fig. 10. Although the volume vanishes for $\nu \to 0$, the surface $S = 2\pi r_{\mathrm{eq}}^2$ and the mean radius of curvature $\tilde{R} = \pi r_{\mathrm{eq}}/4$ are finite.

Since in the limit $\nu \to 0^+$ the volume of all oblate geometries is proportional to ν, the reduced second virial coefficients

FIG. 9. Oblate solids of revolution with an aspect ratio of $\nu = 1/2$. From left to right a double cone, a lens, an ellipsoid, and a cylinder are displayed. All shapes to the left of a given geometry are strict subsets of their right neighbors. The lens and the ellipsoid approach in the limit $\nu \to 1$ a sphere. While a lens does only exist with aspect ratios $\nu \leq 1$, prolate analogs of double cones, ellipsoids, and cylinders with $\nu > 1$ exist.

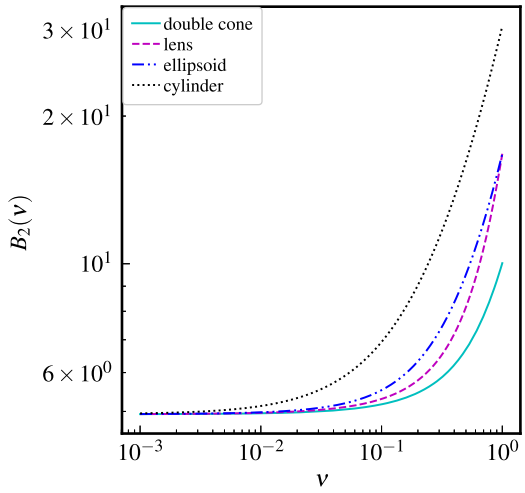

FIG. 10. Second virial coefficients of oblate double cones, lenses, ellipsoids, and cylinders with equatorial radius $r_{eq} = 1$. In the limit $\nu \to 0$, the second virial coefficients of all objects approach the limit $B_2(\nu \to 0) = \pi^2 r_{eq}^3/2$.

diverge as $B_2^*(\nu \to 0^+) \propto \nu^{-1}$. We obtain in the limit $\nu \to 0^+$ the ratios

$$\lim_{\nu\to 0^+} \frac{B_2^{*,(dc)}}{B_2^{*,(ell)}} = 2, \tag{88a}$$

$$\lim_{\nu\to 0^+} \frac{B_2^{*,(lens)}}{B_2^{*,(ell)}} = \frac{4}{3}, \tag{88b}$$

$$\lim_{\nu\to 0^+} \frac{B_2^{*,(cyl)}}{B_2^{*,(ell)}} = \frac{2}{3}, \tag{88c}$$

which are the reciprocal ratios of the volumes for $\nu \to 0^+$. In analogy to the prolate geometries, the geometries with a larger volume exhibit the smallest reduced second virial coefficients in the limit of proportionality $B_2^* \propto \nu^{-1}$.

At the aspect ratio $\nu = 1$, both the lens and the ellipsoid approach a sphere with the identical reduced second virial coefficient $B_2^{*,(lens)}(1) = B_2^{*,(ell)}(1) = 4$. A cylinder

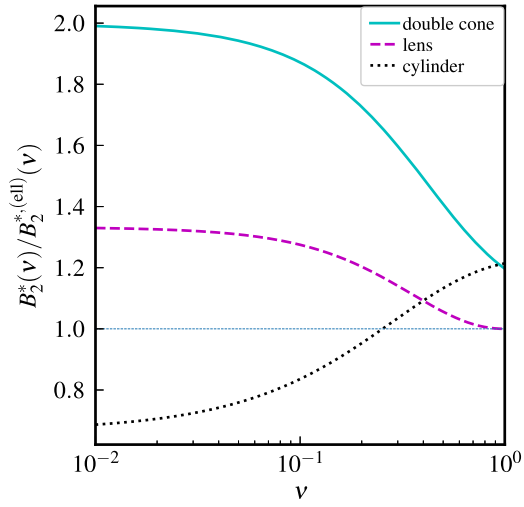

FIG. 11. Reduced second virial coefficients $B_2^*(\nu)$ for double cones, lenses, and cylinders normalized to the second virial coefficient of ellipsoids $B_2^{*,(ell)}(\nu)$ with identical equatorial radius r_{eq}.

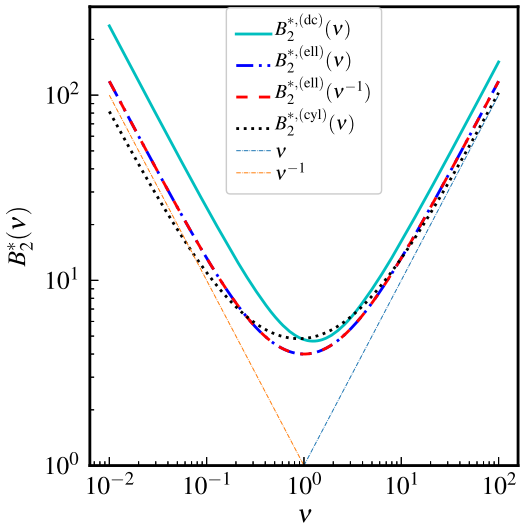

FIG. 12. Reduced second virial coefficients for prolate and oblate double cones, ellipsoids, and cylinders. In the limit $\nu \to \infty$, a proportionality $B_2^*(\nu) \propto \nu$ and in the limit $\nu \to 0^+$, a proportionality $B_2^*(\nu) \propto \nu^{-1}$ is found for all geometries. For ellipsoids, the relation $B_2^{*,(ell)}(\nu) = B_2^{*,(ell)}(\nu^{-1})$ holds.

with an aspect ratio $\nu = 1$ with $B_2^{*,(cyl)}(1) = (3\pi + 10)/16 = 1.214\,049$ has a slightly larger reduced second virial coefficient than a double cone with $B_2^{*,(dc)}(1) = (3\pi + 12)\sqrt{2}/32 + 1/4 = 1.196\,850$. While the ratios $B_2^{*,(dc)}(\nu)/B_2^{*,(ell)}(\nu)$ and $B_2^{*,(lens)}(\nu)/B_2^{*,(ell)}(\nu)$ increase with decreasing aspect ratio, the ratio $B_2^{*,(cyl)}(\nu)/B_2^{*,(ell)}(\nu)$ drops with decreasing aspect ratio.

The reduced second virial coefficient of a cylinder becomes smaller than that of a double cone for $\nu < 0.940\,101$, smaller than that of a lens for $\nu < 0.399\,489$ and smaller than that of an ellipsoid for $\nu < 0.252\,962$ (Fig. 11).

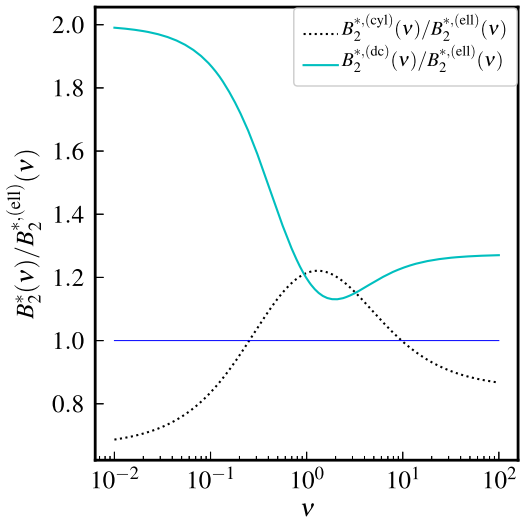

FIG. 13. Reduced second virial coefficients of cylinders and double cones normalized to those of ellipsoids. In the range $0.252\,964 < \nu < 9.731\,169$, the reduced virial coefficients of cylinders exceed those of ellipsoids, while for sufficiently large and sufficiently small aspect ratios, the ratio of excluded volume to particle volume is for cylinders the smallest of the geometries existing both as prolate and oblate objects. For double cones, this ratio is for any aspect ratio larger than for ellipsoids, while in the range $0.9401 < \nu < 3.2317$, this ratio is for cylinders even larger than for double cones.

Double cones, ellipsoids, and cylinders exist both as prolate and oblate solids of revolution. For ellipsoids, the symmetry relation $B_2^{*,(\mathrm{ell})}(\nu) = B_2^{*,(\mathrm{ell})}(1/\nu)$ is found as visible in Fig. 12. The reduced second virial coefficient of a double cone is for any aspect ratio larger than that of an ellipsoid. For sufficiently large and sufficiently small aspect ratios, the reduced second virial coefficients of cylinders are smaller than those of ellipsoids, while in the range $0.252\,964 < \nu < 9.731\,169$, the virial coefficients of cylinders exceed those of ellipsoids. In the range $0.940\,101 < \nu < 3.231\,733$, $B_2^{*,(\mathrm{cyl})}$ exceeds $B_2^{*,(\mathrm{dc})}$ (Fig. 13).

V. CONCLUSIONS

Employing the Isihara–Hadwiger theorem, analytical expressions for the second virial coefficient can be derived for various convex geometries with hard-body interaction. The geometric measures needed to calculate these second virial coefficients are compiled in Tables I and II. Singularities in the surface curvature can be removed for convex solids of revolution when the meridian curve in the vicinity of a singularity is continuously completed by those of segments of spheres or ellipsoids. Ellipsoids and spheres, as ellipsoids with an aspect ratio $\nu = 1$, are continuous with respect to the curvature at the entire particle surface. The influence of a singularity is obtained in the limit of infinitely small spheres or infinitely thin ellipsoids.

Apices as one-dimensional singularities located at the symmetry axis of solids of revolution do not contribute to the mean radius of curvature. In contrast, the contribution of two-dimensional singularities is the product of the singularity's radius and the angle $(\pi - \zeta)/4$, where ζ is the angle enclosed between the tangents at both sides of the singularity.

Beyond the influence of the aspect ratio, the virial coefficients of hard solids of revolution depend on the detailed geometry of the particles. The reduced second virial coefficients of all geometries show a proportionality $B_2^*(\nu \to \infty) \propto \nu$ with constant ratios between different geometries in the limit of infinitely large aspect ratios. The same holds for oblate geometries in the limit $\nu \to 0^+$, however, with a proportionality $B_2^*(\nu \to 0^+) \propto \nu^{-1}$. Hence, even in the limit of very large or very small aspect ratios, the detailed geometry leads to significantly different orientational averages of the mutual excluded volume.

The aim of future work will be to calculate higher virial coefficients of hard ellipsoids and spindles in dependence on their aspect ratio. A suitable and efficient approach is the Mayer-sampling Monte Carlo method.[36,37]

TABLE I. Geometric measures for centrosymmetric solids of revolution.

Ellipsoid prolate ($\nu \geq 1$)	$V = \frac{4\pi}{3}\nu^{(\mathrm{ell})} r_{\mathrm{eq}}^{3,(\mathrm{ell})}$	$S = \frac{2\pi r_{\mathrm{eq}}^{2,(\mathrm{ell})}}{\left(\nu^{2,(\mathrm{ell})}-1\right)^{1/2}}\left[\nu^{2,(\mathrm{ell})}\arcsin\left(\frac{\left(\nu^{2,(\mathrm{ell})}-1\right)^{1/2}}{\nu^{(\mathrm{ell})}}\right)+\left(\nu^{2,(\mathrm{ell})}-1\right)^{1/2}\right]$ $\tilde{R} = \frac{\nu^{(\mathrm{ell})} r_{\mathrm{eq}}^{(\mathrm{ell})}}{2} + \frac{r_{\mathrm{eq}}^{(\mathrm{ell})}}{2\left(\nu^{2,(\mathrm{ell})}-1\right)^{1/2}}\operatorname{arctanh}\left(\frac{\left(\nu^{2,(\mathrm{ell})}-1\right)^{1/2}}{\nu^{(\mathrm{ell})}}\right)$
Ellipsoid oblate ($\nu \leq 1$)	$V = \frac{4\pi}{3}\nu^{(\mathrm{ell})} r_{\mathrm{eq}}^{3,(\mathrm{ell})}$	$S = \frac{2\pi r_{\mathrm{eq}}^{2,(\mathrm{ell})}}{\left(1-\nu^{2,(\mathrm{ell})}\right)^{1/2}}\left[\nu^{2,(\mathrm{ell})}\ln\left(\frac{1+\left(1-\nu^{2,(\mathrm{ell})}\right)^{1/2}}{\nu^{(\mathrm{ell})}}\right)+\left(1-\nu^{2,(\mathrm{ell})}\right)^{1/2}\right]$ $\tilde{R} = \frac{\nu^{(\mathrm{ell})} r_{\mathrm{eq}}^{(\mathrm{ell})}}{2} + \frac{r_{\mathrm{eq}}^{(\mathrm{ell})}}{2\left(1-\nu^{2,(\mathrm{ell})}\right)^{1/2}}\arctan\left(\frac{\left(1-\nu^{2,(\mathrm{ell})}\right)^{1/2}}{\nu^{(\mathrm{ell})}}\right)$
Spherocylinder	$V = 2\pi r_{\mathrm{eq}}^{3,(\mathrm{sc})}\left(\nu^{(\mathrm{sc})} - \frac{1}{3}\right)$	$S = 4\pi r_{\mathrm{eq}}^{2,(\mathrm{sc})}\nu^{(\mathrm{sc})}$ $\tilde{R} = \frac{\nu^{(\mathrm{sc})}+1}{2} r_{\mathrm{eq}}^{(\mathrm{sc})}$
Spindle	$V = \frac{\pi r_{\mathrm{eq}}^{3,(\mathrm{sp})}}{12}\left[6\nu^{5,(\mathrm{sp})}+4\nu^{3,(\mathrm{sp})}+6\nu^{(\mathrm{sp})}-3\left(\nu^{6,(\mathrm{sp})}+\nu^{4,(\mathrm{sp})}-\nu^{2,(\mathrm{sp})}-1\right)\times\arcsin\left(\frac{2\nu^{(\mathrm{sp})}}{\nu^{2,(\mathrm{sp})}+1}\right)\right]$	$S = 2\pi r_{\mathrm{eq}}^{2,(\mathrm{sp})}\left[\nu^{(\mathrm{sp})}\left(\nu^{2,(\mathrm{sp})}+1\right)+\frac{1-\nu^{4,(\mathrm{sp})}}{2}\arcsin\left(\frac{2\nu^{(\mathrm{sp})}}{\nu^{2,(\mathrm{sp})}+1}\right)\right]$ $\tilde{R} = r_{\mathrm{eq}}^{(\mathrm{sp})}\left[\nu^{(\mathrm{sp})} - \frac{\nu^{2,(\mathrm{sp})}-1}{4}\arcsin\left(\frac{2\nu^{(\mathrm{sp})}}{\nu^{2,(\mathrm{sp})}+1}\right)\right]$
Lens	$V = \pi r_{\mathrm{eq}}^{3,(\mathrm{lens})}\left(\nu^{(\mathrm{lens})} + \frac{\nu^{3,(\mathrm{lens})}}{3}\right)$	$S = 2\pi r_{\mathrm{eq}}^{2,(\mathrm{lens})}\left(1+\nu^{2,(\mathrm{lens})}\right)$ $\tilde{R} = r_{\mathrm{eq}}^{(\mathrm{lens})}\left[\nu^{(\mathrm{lens})} + \frac{1}{2}\arctan\left(\frac{1-\nu^{2,(\mathrm{lens})}}{2\nu^{(\mathrm{lens})}}\right)\right]$
Double cone	$V = \frac{2}{3}\pi\nu^{(\mathrm{dc})} r_{\mathrm{eq}}^{3,(\mathrm{dc})}$	$S = 2\pi\left(1+\nu^{2,(\mathrm{dc})}\right)^{1/2} r_{\mathrm{eq}}^{2,(\mathrm{dc})}$ $\tilde{R} = \frac{r_{\mathrm{eq}}}{2}\left[\nu^{(\mathrm{dc})} + \arctan\left(\frac{1}{\nu^{(\mathrm{dc})}}\right)\right]$
Cylinder	$V = 2\pi r_{\mathrm{eq}}^{3,(\mathrm{cyl})}\nu^{(\mathrm{cyl})}$	$S = 2\pi r_{\mathrm{eq}}^{2,(\mathrm{cyl})}\left(1+2\nu^{(\mathrm{cyl})}\right)$ $\tilde{R} = \left(\frac{\nu^{(\mathrm{cyl})}}{2} + \frac{\pi}{4}\right) r_{\mathrm{eq}}^{(\mathrm{cyl})}$

TABLE II. Geometric measures for solids of revolution without inversion symmetry.

Cone	$V = \frac{\pi}{3}\nu^{(c)} r_0^{3,(c)}$	$S = \pi\left[1 + \left(1+\nu^{2,(c)}\right)^{1/2}\right] r_0^{2,(c)}$ $\tilde{R} = \frac{r_0^{(c)}}{4}\left[\nu^{(c)} + \frac{\pi}{2} + \arctan\left(\frac{1}{\nu^{(c)}}\right)\right]$
Truncated cone	$V = \pi h\left[r_0^{2,(tc)} - \frac{h r_0^{(tc)}}{\nu^{(tc)}} + \frac{1}{3}\left(\frac{h}{\nu^{(tc)}}\right)^2\right]$ $\nu^{(tc)} = \frac{h}{r_0^{(tc)} - r_1} \qquad \xi = \arctan\left(\frac{1}{\nu^{(tc)}}\right)$	$S = \pi\left[1 - \left(1+\nu^{2,(tc)}\right)^{1/2}\right]\left[\left(\frac{h}{\nu^{(tc)}}\right)^2 - 2r_0^{(tc)}\frac{h}{\nu^{(tc)}}\right] + 2\pi r_0^{2,(tc)}$ $\tilde{R} = \frac{h}{4} + \frac{r_0^{(tc)}}{4}\left(\frac{\pi}{2}+\xi\right) + \frac{r_1}{4}\left(\frac{\pi}{2}-\xi\right)$
Sphere segment ($h \le r_0^{(seg)}$)	$V = \frac{\pi r_0^{3,(seg)}}{2}\left(\nu^{(seg)} + \frac{\nu^{3,(seg)}}{3}\right)$ $\nu^{(seg)} = \frac{h}{r_0^{(seg)}}$	$S = \pi r_0^{2,(seg)}\left(1+\nu^{2,(seg)}\right)$ $\tilde{R} = \frac{r_0^{(seg)}}{2}\left[\nu^{(seg)} + \frac{\pi}{4} + \frac{1}{2}\arctan\left(\frac{1-\nu^{2,(seg)}}{2\nu^{(seg)}}\right)\right]$
Sphere segment ($h \ge r_0^{(seg)}$)	$V = \frac{4\pi r_0^3}{3} - \frac{\pi r_0^{3,(seg)}}{2}\left(\nu^{(seg)} + \frac{\nu^{3,(seg)}}{3}\right)$ $r_0 = \frac{\nu^{(seg)} r_0^{(seg)} + h}{2}$	$S = 4\pi r_0^2 - \pi r_0^{2,(seg)}\left(1+\nu^{2,(seg)}\right)$ $\tilde{R} = r_0 - \frac{r_0^{(seg)}}{4}\left[\frac{\pi}{2} - \nu^{(seg)} - \arctan\left(\frac{1-\nu^{2,(seg)}}{2\nu^{(seg)}}\right)\right]$

SUPPLEMENTARY MATERIAL

See supplementary material for details concerning a double cone's mean radius of curvature (Sec. S-I) and for the second virial coefficients of solids of revolution without inversion symmetry such as cones, truncated cones, and sphere segments (Sec. S-II).

APPENDIX A: CONTINUOUS COMPLETION OF A TRUNCATED SPINDLE

Using Eqs. (54) and (55), at $z = \nu r_{eq} - \varepsilon$, the equatorial radius $r_{eq}^{(sph)}$ and center z_0 of the sphere, Eq. (56), are related by

$$r_{eq}^{(sph)} = r_{eq}^{(sp)}\frac{\nu^2+1}{2}\left\{1 + \frac{r_{eq}^{(sp)}\left(1-\nu^2\right)}{\left[\left(\nu^2+1\right)^2 r_{eq}^{2,(sp)} - 4z'^2\right]^{1/2}}\right\} \quad \text{(A1)}$$

with $z' = \nu r_{eq}^{(sp)} - \varepsilon$. The sphere's center is located at

$$z_0 = r_{eq}^{(sp)}\frac{\left(\nu^2-1\right)z'}{\left[\left(\nu^2+1\right)^2 r_{eq}^{2,(sp)} - 4z'^2\right]^{1/2}}. \quad \text{(A2)}$$

In the limit $\varepsilon \to 0$, i.e., $z' \to \nu r_{eq}^{(sp)}$, we obtain

$$\lim_{z' \to \nu r_{eq}^{(sp)}} r_{eq}^{(sph)} = 0 \quad \text{(A3)}$$

and

$$\lim_{z' \to \nu r_{eq}^{(sp)}} z_0(z') = \nu r_{eq}^{(sp)}. \quad \text{(A4)}$$

APPENDIX B: CONTINUOUS COMPLETION OF A CUT-OUT LENS

Using Eqs. (68), the aspect ratio of an ellipsoid which continuously completes a lens with the equatorial radius $r_{eq}^{(lens)}$ and the aspect ratio $\nu^{(lens)}$ cut out for $-\varepsilon \le z \le \varepsilon$ is

$$\nu^{(ell)} = \frac{\left\{2\nu^{(lens)}\varepsilon\left[2\nu^{(lens)}\varepsilon - \left(\nu^{2,(lens)}-1\right)r_{eq}^{(lens)}\right]\right\}^{1/2}}{\left(\nu^{2,(lens)}-1\right)r_{eq}^{(lens)} - 2\nu^{(lens)}\varepsilon}. \quad \text{(B1)}$$

Its equatorial radius can be written as

$$r_{eq}^{(ell)} = \frac{1}{2}\left\{\frac{2r_{eq}^{(lens)}\left[2\nu^{(lens)}r_{eq}^{(lens)}\left(\nu^{2,(lens)}-1\right)\varepsilon\right]}{\nu^{(lens)}}\right\}^{1/2}. \quad \text{(B2)}$$

With $\nu^{(ell)}$ and $r_{eq}^{(ell)}$, the contribution of the continuous completion to the mean radius of curvature, Eq. (69), can be expressed as

$$\begin{aligned}\tilde{R}'^{(lens)} = \frac{1}{2\lambda}\Big\{&\arctan\left(\frac{\kappa}{\lambda}\right)\Big[2r_{eq}^{2,(lens)}\nu^{(lens)}\left(\nu^{2,(lens)}-1\right) \\ &+ \varepsilon r_{eq}^{(lens)}\left(\nu^{4,(lens)} - 6\nu^{2,(lens)} + 1\right) \\ &- 2\varepsilon^2\nu^{(lens)}\left(\nu^{2,(lens)}-1\right)\Big]\Big\} + \frac{\varepsilon}{2}\end{aligned} \quad \text{(B3)}$$

with the abbreviations

$$\kappa = 2\varepsilon\nu^{(lens)}\left(\nu^{2,(lens)}-1\right) - r_{eq}^{(lens)}\left(\nu^{2,(lens)}-1\right)^2 \quad \text{(B4a)}$$

and

$$\begin{aligned}\lambda = \Big\{&2\nu^{(lens)}\left(1-\nu^{2,(lens)}\right)\Big[2\nu^{(lens)}\left(1-\nu^{2,(lens)}\right)r_{eq}^{2,(lens)} \\ &- \varepsilon\left(\nu^{4,(lens)} - 6\nu^{2,(lens)} + 1\right)r_{eq}^{(lens)} \\ &- 2\varepsilon^2\nu^{(lens)}\left(1-\nu^{2,(lens)}\right)\Big]\Big\}^{1/2}.\end{aligned} \quad \text{(B4b)}$$

In the limit $\varepsilon \to 0$, one obtains

$$\lim_{\varepsilon\to 0}\tilde{R}'^{(lens)} = \frac{r_{eq}^{(lens)}}{2}\arctan\left(\frac{1-\nu^{2,(lens)}}{2\nu^{(lens)}}\right). \quad \text{(B5)}$$

[1] H. Kamerlingh Onnes, P. K. Akad. Wetensc. **4**, 125 (1902).
[2] J.-P. Hansen and L. Verlet, Phys. Rev. **184**, 151 (1969).
[3] C. G. Gray and K. E. Gubbins, *Theory of Molecular Liquids* (Clarendon Press, 1984).
[4] J. A. Barker and D. Henderson, Rev. Mod. Phys. **48**, 587 (1976).

[5]Y. Singh, Phys. Rep. **207**, 351 (1991).
[6]H. Löwen, J. Phys.: Condens. Matter **14**, 11897 (2002).
[7]N. F. Carnahan and K. E. Starling, J. Chem. Phys. **51**, 635 (1969).
[8]A. Poniewierski and R. Hołyst, Phys. Rev. Lett. **61**, 2461 (1988).
[9]R. Hołyst and A. Poniewierski, Phys. Rev. A **39**, 2742 (1989).
[10]H. Graf and H. Löwen, Phys. Rev. E **59**, 1932 (1999).
[11]L. Onsager, Ann. N. Y. Acad. Sci. **51**, 627 (1949).
[12]A. Isihara, J. Chem. Phys. **18**, 1446 (1950).
[13]T. Boublík and I. Nezbeda, Collect. Czech. Chem. Commun. **51**, 2301 (1986).
[14]D. Frenkel, B. M. Mulder, and J. P. McTague, Phys. Rev. Lett. **52**, 287 (1984).
[15]P. Bolhuis and D. Frenkel, Phys. Rev. Lett. **72**, 2211 (1994).
[16]P. G. Bolhuis, A. Stroobants, D. Frenkel, and H. N. W. Lekkerkerker, J. Chem. Phys. **107**, 1551 (1997).
[17]J. A. C. Veerman and D. Frenkel, Phys. Rev. A **45**, 5632 (1992).
[18]D. van der Beek and H. N. W. Lekkerkerker, Langmuir **20**, 8582 (2004).
[19]M. Ozaki, S. Kratohvil, and E. Matijevic, J. Colloid Interface Sci. **102**, 146 (1984).
[20]C. Märkert, B. Fischer, and J. Wagner, J. Appl. Crystallogr. **44**, 441 (2011).
[21]J. E. G. J. Wijnhoven, D. van't Zand, D. van der Beek, and H. N. W. Lekkerkerker, Langmuir **21**, 10422 (2005).
[22]J. E. G. J. Wijnhoven, J. Colloid Interface Sci. **292**, 403 (2005).
[23]R. Zhang and K. S. Schweizer, J. Chem. Phys. **136**, 154902 (2012).
[24]J. Henzie, M. Grünwald, A. Widmer-Cooper, P. L. Geissler, and P. Yang, Nat. Mater. **11**, 131 (2012).
[25]A. Donev, F. H. Stillinger, P. M. Chaikin, and S. Torquato, Phys. Rev. Lett. **92**, 255506 (2004).
[26]S. Torquato and Y. Jiao, Nature **460**, 876 (2009).
[27]G. Odriozola, M. Romero-Bastida, and F. de J. Guevara-Rodríguez, Phys. Rev. E **70**, 021405 (2004).
[28]G. Odriozola, J. Chem. Phys. **136**, 134505 (2012).
[29]M. Á. G. Maestre, A. Santos, M. Robles, and M. L. de Haro, J. Chem. Phys. **134**, 084502 (2011).
[30]M. E. Irrgang, M. Engel, A. J. Schultz, D. A. Kofke, and S. C. Glotzer, Langmuir **33**, 11788 (2017).
[31]C. Vega, Mol. Phys. **92**, 651 (1997).
[32]A. Isihara and T. Hayashida, J. Phys. Soc. Jpn. **6**, 40 (1951).
[33]A. Isihara and T. Hayashida, J. Phys. Soc. Jpn. **6**, 46 (1951).
[34]H. Hadwiger, Experientia **7**, 395 (1951).
[35]The expression of the mean radius of curvature in Table I of Ref. 13 is actually an expansion of the exact formulation (77) for large aspect ratios, which leads to unphysical results in the limit $\nu \to 0$.
[36]J. K. Singh and D. A. Kofke, Phys. Rev. Lett. **92**, 220601 (2004).
[37]C. Zhang and B. M. Pettitt, Mol. Phys. **112**, 1427 (2014).